AD-A045 119 ARMY COMMUNICATIONS-ELECTRONICS ENGINEERING INSTALLAT--ETC F/G 17/2.1
DEB STAGE 1 - CONUS LINK TESTING.(U)
JUL 77 J E HAMANT, R G CATTS, S T SCHOCH
UNCLASSIFIED CCC-CED-77-DTEP-015 NL

| OF |
AD A045 119

END
DATE FILMED
11-77
DDC

(14) CCC-CED-77-DTEP-015

(8) (15) B.S.

(6) DEB STAGE 1 - CONUS LINK TESTING.

(9) Final rept. May 76 - May 77,

(10) CPT JAMES E. HAMANT
CPT RANDALL G. CATTS
MSG STEPHEN T. SCHOCH
MR. OWEN P. CONNELL
MR. GAIL QUERY
MR. ROBERT S. STEELE

(11) JULY 1977

(12) 84p.

HEADQUARTERS
US ARMY COMMUNICATIONS-ELECTRONICS ENGINEERING INSTALLATION AGENCY
Fort Huachuca, Arizona 85613

1473

405 982

LB

UNCLASSIFIED

SECURITY CLASSIFICATION OF THIS PAGE (When Data Entered)

REPORT DOCUMENTATION PAGE		READ INSTRUCTIONS BEFORE COMPLETING FORM
1. REPORT NUMBER CCC-CED-76-DTEP-015	2. GOVT ACCESSION NO.	3. RECIPIENT'S CATALOG NUMBER
4. TITLE (and Subtitle) DEB Stage 1 CONUS LINK TESTING		5. TYPE OF REPORT & PERIOD COVERED Final Report May 1976 - May 1977
		6. PERFORMING ORG. REPORT NUMBER CCC-CED-76-DTEP-015
7. AUTHOR(s) CPT James E. Hamant; MSG Stephen T. Schoch Mr. Owen P. Connel; Mr. Robert S. Steele CPT Randall G. Catts, USAEPG; Gail Query, USAEPG		8. CONTRACT OR GRANT NUMBER(s)
9. PERFORMING ORGANIZATION NAME AND ADDRESS US Army Communications-Electronics Engineering Installation Agency and US Army Electronic Proving Ground, Fort Huachuca, Arizona 85613		10. PROGRAM ELEMENT, PROJECT, TASK AREA & WORK UNIT NUMBERS
11. CONTROLLING OFFICE NAME AND ADDRESS U.S. Army Communications Command, DCSOPS, Vice Assistant Chief of Staff for Force Development, Fort Huachuca, Arizona 85613		12. REPORT DATE July 1977 13. NUMBER OF PAGES 83
14. MONITORING AGENCY NAME & ADDRESS(if different from Controlling Office) US Army Communications Systems Agency Fort Monmouth, NJ 07703		15. SECURITY CLASS. (of this report) UNCLASSIFIED 15a. DECLASSIFICATION/DOWNGRADING SCHEDULE

16. DISTRIBUTION STATEMENT (of this Report)

Approved for public release, distribution unlimited.

17. DISTRIBUTION STATEMENT (of the abstract entered in Block 20, if different from Report)

18. SUPPLEMENTARY NOTES

To be entered in Defense Documentation Center.

19. KEY WORDS (Continue on reverse side if necessary and identify by block number)

microwave communications
digital transmission
3-level partial response
duo-binary
biternary

20. ABSTRACT (Continue on reverse side if necessary and identify by block number)

CONUS link testing was initiated to establish a data base and performance assessment of a similar microwave system in advance of the final implementation of the DEB Stage-1 program. Six AN/FRC 162 radios, two AN/FRC 165 radios, and ten T1-4000 multiplexers were used to establish four terminals with the capability of propagating over eight paths, one of which had a length of 82 miles. Long term results show a close correlation of measured and predicted signal levels. A large difference was noted in the number of fades recorded at each terminal receiver, over one path. The BER was 1.85×10^{-8} after eight transmission links

DD FORM 1 JAN 73 1473 EDITION OF 1 NOV 65 IS OBSOLETE

UNCLASSIFIED

SECURITY CLASSIFICATION OF THIS PAGE (When Data Entered)

of baseband repeaters. Variability among multiplexer sensitivities was important in determining the distribution of errors in the baseband repeater tests. A Baseband Degradation Monitor was found to be suitable for use on a one hop transmission system.

TABLE OF CONTENTS

PARAGRAPH		PAGE
1.	BACKGROUND	
1.1	Introduction	1
1.2	Approach to the Task	1
1.3	General Test Objectives	7
1.4	Summary of Findings	7
2.	GENERAL	
2.1	Description of Equipment	8
2.2	Summary of AN/FRC-162 Test Results	8
2.3	Test Methodology and Limitations	9
2.4	Unscheduled Test Observations	12
3.	DETAILS OF TESTING	
3.1	Received Signal Levels: Predicted vs Actual	13
3.2	Path Fading	18
3.3	Bit Error Rate	19
3.4	Baseband Repeater Operation	22
3.5	Multiplexer Performance	30
3.6	Baseband Degradation Monitor	31
3.7	Cross Polarization	38
3.8	Wideband Noise Quieting	41
3.9	Noise Power Ratio	52

TABLE OF CONTENTS (cont)

APPENDICES	PAGE
A. Terminal Equipment Specifications	63
B. Mule Mountain - Mount Lemmon Path Profiles	64
C. Automated Data Collection System	67

LIST OF ILLUSTRATIONS

FIGURE		PAGE
1.	Simplified Map: DEB CONUS Link Configuration	2
2.	Photograph of Mount Lemmon Microwave Site	3
3.	Photograph of Mule Mountain Microwave Site	4
4.	Photograph of Site Sibyl	5
5.	Photograph of CTA Microwave Site	6
6.	AN/FRC-162 Bit Error Rate vs Received Signal Level Characteristic Curves	10
7.	AN/FRC-162 Bit Error Rate vs Unavailability	11
8.	Test Configuration for Received Signal Level Measurements	15
9.	Sample RSL Availability	16
10.	Predicted vs Actual Received Signal Level Relationship	17
11.	Test Configuration for Baseband Repeater Operation	23
12.	Eight-Hop Transmission Diagrams	24
13.	Baseband Frequency Response Characteristics for Eight-Hop Transmission	25
14.	Baseband Frequency Response Characteristics for 1, 2, 3, and 4-Hop Transmission	26
15.	Oscillographs of Eye Patterns for Baseband Repeater Operation	27
16.	Oscillographs of Sequential Baseband Spectra Part I	28
16.	Oscillographs of Sequential Baseband Spectra Part II	29

LIST OF ILLUSTRATIONS (cont)

FIGURE		PAGE
17.	Test Configuration for Baseband Degradation Monitor	32
18.	Typical Response Curve for BDM	34
19.	Normal Distribution for "0" and "1"	35
20.	BDM Response for CTA - MMT Link	36
21.	BDM Response for Six Hops	37
22.	Multi-Hop BDM Response	39
23.	Test Configuration for Cross Polarization Test	40
24.	Cross Polarization Distribution for MMT	42
25.	Cross Polarization Distribution for MTL	43
26.	Faded Link Cross Polarization Isolation MTL	44
27.	Faded Link Cross Polarization Isolation MMT	45
28.	Test Configuration for Wideband Noise Quieting	46
29.	Noise Quieting Curve for 70 KHz Slot	47
30.	Noise Quieting Curve for 1248 KHz Slot	48
31.	Noise Quieting Curve for 2438 KHz Slot	49
32.	Noise Quieting Curve for 3886 KHz Slot	50
33.	Noise Quieting Curve for 5340 KHz Slot	51
34.	Multiplex Response at Q6	53
35.	Multiplex Response at High Pass Filter	54
36.	Noise Power Ratio vs Noise Load	57
37.	Expanded Noise Power Ratio vs Noise Load	58

LIST OF ILLUSTRATIONS (cont)

FIGURE		PAGE
38.	Noise Power Ratio vs Noise Load for 60 to 5340 KHz	59
39.	Mule Mountain - Mount Lemmon Path Profile (K=4/3)	64
40.	Mule Mountain - Mount Lemmon Path Profile (K=3/3)	65
41.	Mule Mountain - Mount Lemmon Path Profile (K=2/3)	66
42.	Photograph of Calculator System	68
43.	Calculator Interface	69
44.	Flow Chart: Data Acquisition Program Part I	71
45.	Flow Chart: Data Acquisition Program Part II	72
46.	Flow Chart: Data Acquisition Program Part III	73
47.	Flow Chart: Data Reduction Program Part I	74
48.	Flow Chart: Data Reduction Program Part II	75
49.	Photograph of Calculator System	76

LIST OF TABLES

TABLE		PAGE
1.	Microwave Paths and Lengths	1
2.	Long Link Fades	19
3.	MMT Error Distribution	20
4.	MTL Error Distribution	21
5.	Baseband Repeater Performance	30
6.	Comparisons of Measured and Calculated S/N	61
7.	minal Equipment Specifications	63

1. BACKGROUND

1.1 Introduction.

1.1.1 This document reports the results of tests performed on the Defense Communication System (DCS) microwave radio system modified for three-level partial response, operated over multiple-hop microwave links. The US Army Communications-Electronics Engineering Installation Agency (USACEEIA) was assigned the task of establishing a four-path microwave complex, including an 80-mile line-of-sight link to collect propagation and system engineering data in support of the Digital European Backbone (DEB) Stage I Program. This system was tested as part of the US Army Communications Command (USACC) Digital Transmission Evaluation Project (DTEP) during the period of May 1976 to May 1977.

1.1.2 USACEEIA was authorized to perform this mission by Department of the Army message, DAMO-TSC-T, 272145Z Jun 75; and US Army Communications Systems Agency (USACSA) message, CCM-SP-C, 251936Z Jul 75. USACSA, Fort Monmouth, New Jersey is responsible for managing the DTEP. Conduct of the tests was tasked to the US Army Electronic Proving Ground (USAEPG), Fort Huachuca, Arizona under the technical guidance and supervision of USACEEIA, Fort Huachuca, Arizona.

1.2 Approach to the Task.

1.2.1 Some DEB microwave links exceed 50 miles in length and cover mountainous terrain. To simulate this condition work was initiated in July 1975 and completed in May 1976 establishing a four link configuration with terminals at Mount Lemmon near Tucson, Arizona; Mule Mountain near Bisbee, Arizona, Fort Huachuca (CTA) and Site Sibyl near Benson, Arizona. Figure 1 is a simplified map which illustrates the geometrical and topographic configurations of the four terminals. Table 1 lists the four microwave paths and their respective lengths in miles. Figures 2 through 5 are photographs of each of the four terminals used in this study.

Table 1. Microwave Paths and Lengths

PATH	DISTANCE
CTA - Site Sibyl	32.1 miles
Site Sibyl - Mount Lemmon	47.3 miles
Mule Mountain - Mount Lemmon	82.0 miles
Mule Mountain - CTA	23.7 miles

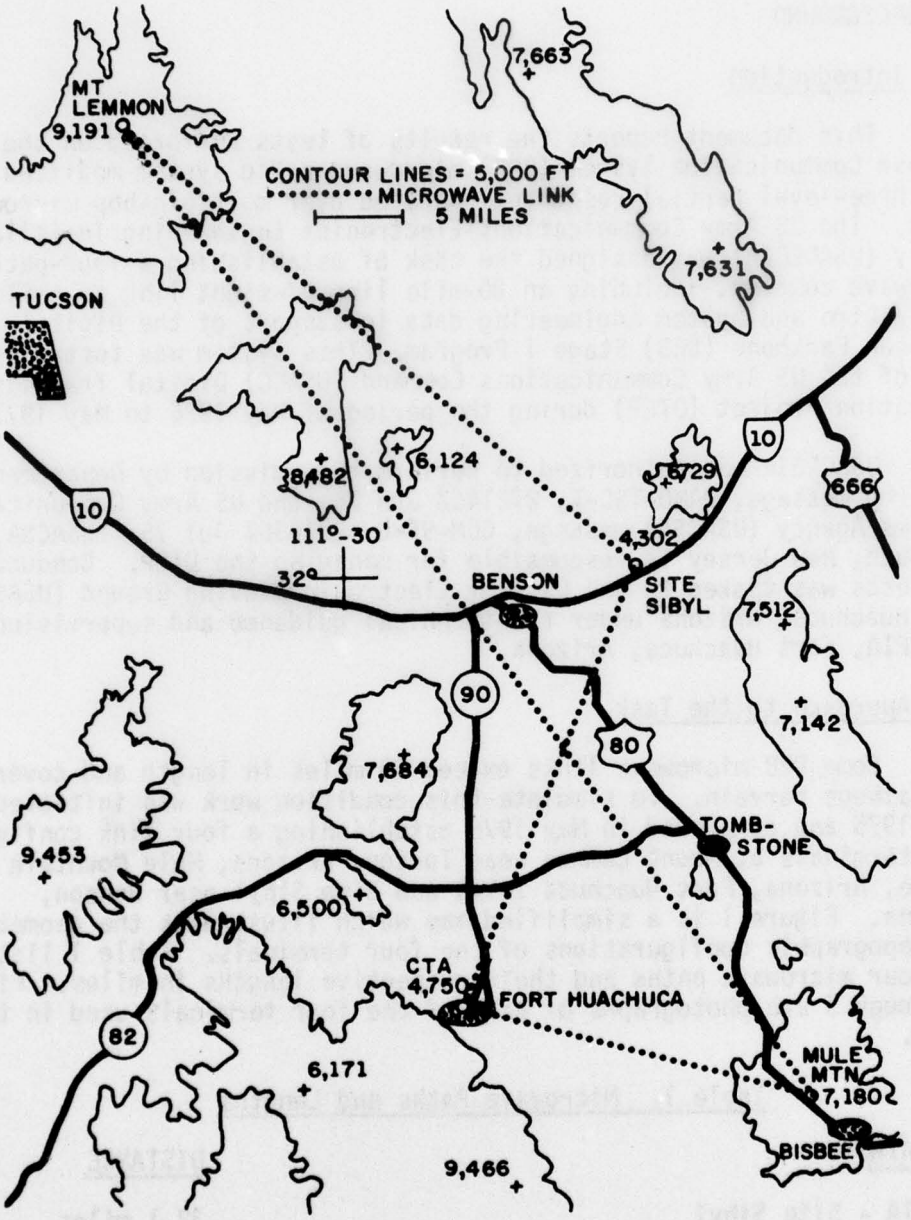

Figure 1. Simplified Map: DEB CONUS Link Configuration

Figure 2. Photograph of Mount Lemmon Microwave Site

Figure 3. Photograph of Mule Mountain Microwave Site

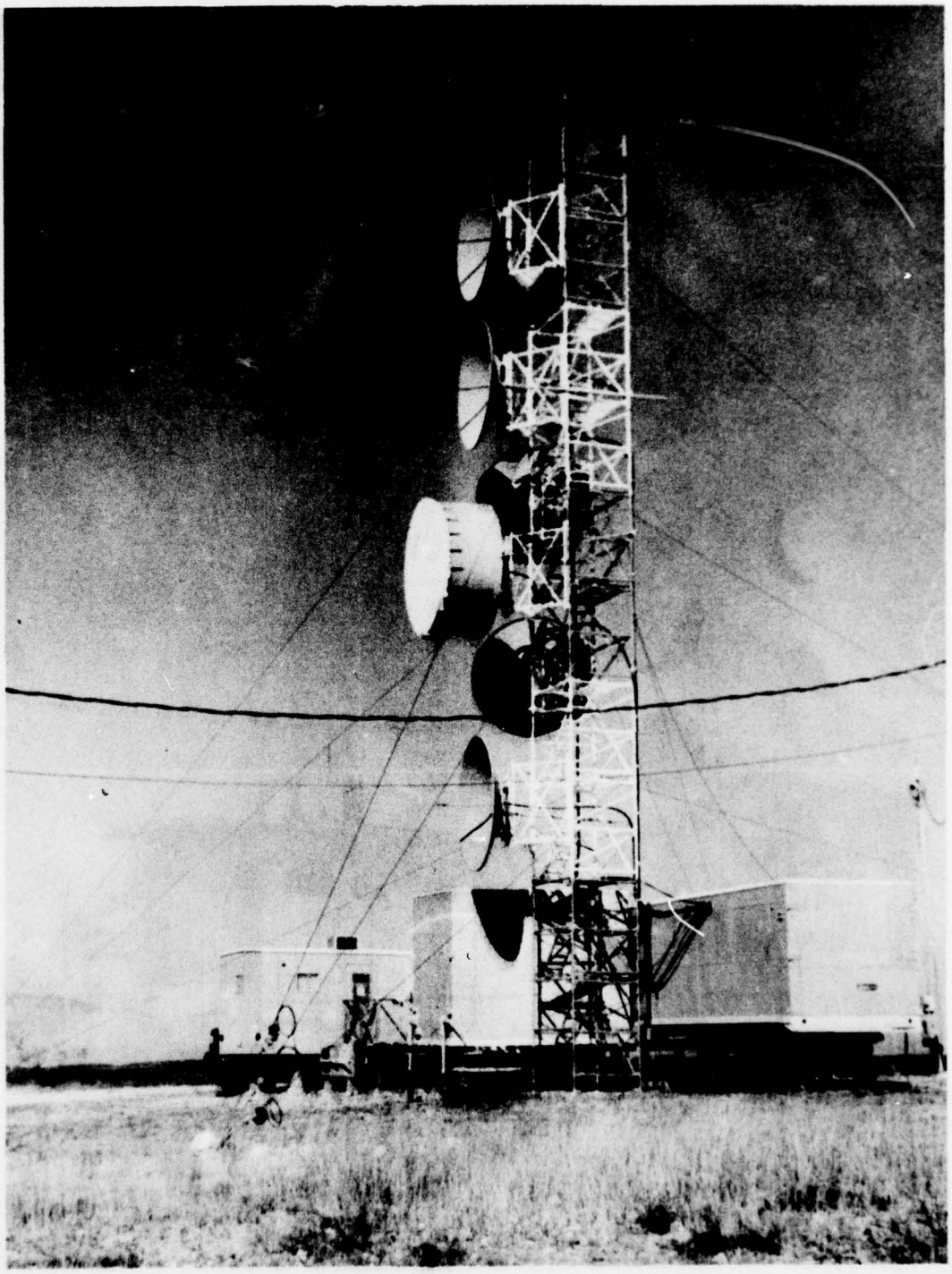

Figure 4. Photograph of Site Sibyl

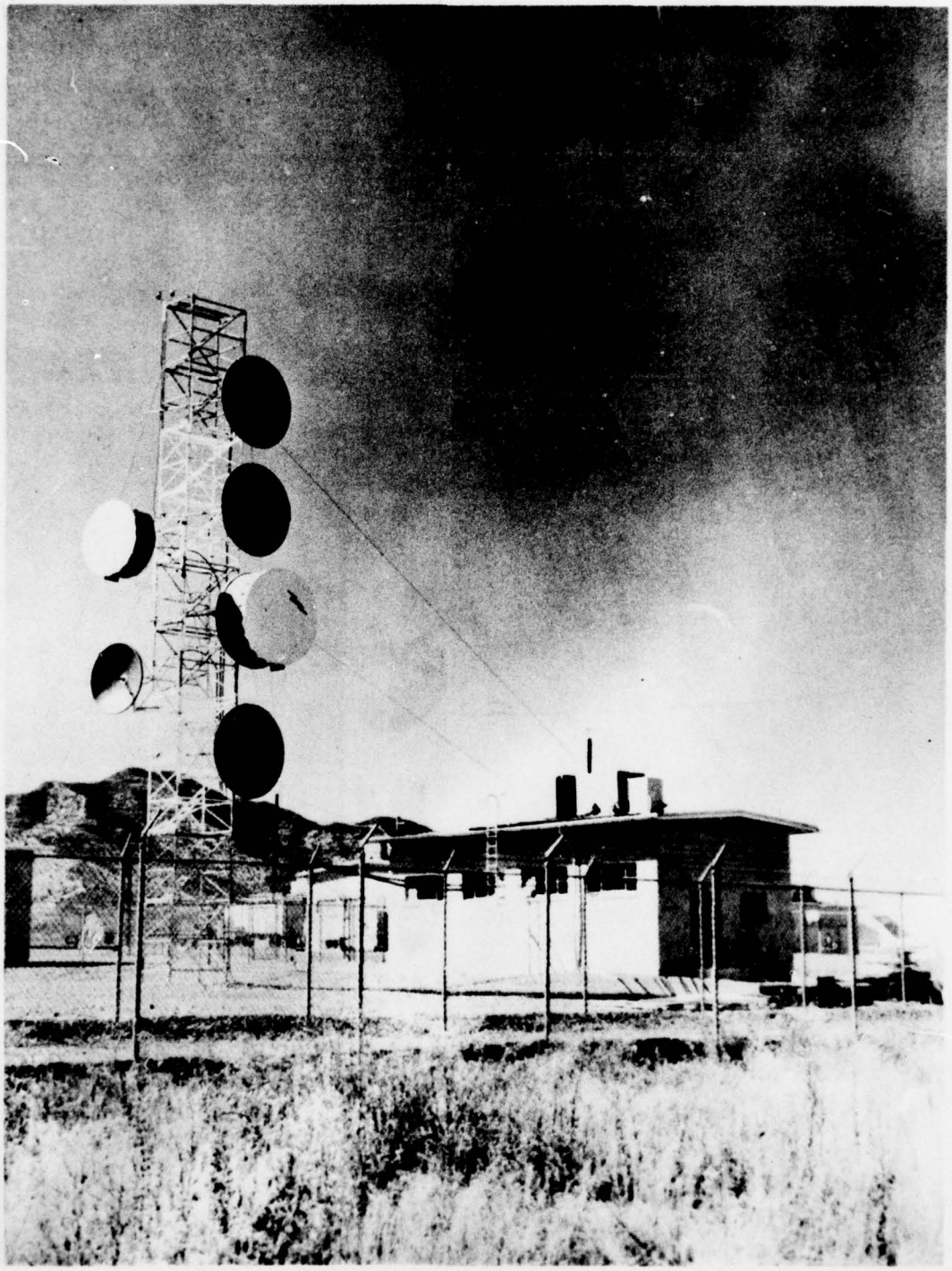

Figure 5. Photograph of CTA Microwave Site

1.2.2 To establish the priorities of engineering and testing, the areas of investigation were initially divided into four categories. Category I included data collection and preliminary engineering analysis of received signal levels (RSL's), fade margins, fade depths, fade rates, fade durations, bit error rate (BER) vs RSL, multiplexer reframes, and baseband repeater operation. Category II included data collection and engineering analysis of cross-polarization, space diversity receiver switching and three-level logic violations, as well as final engineering analysis of long-term studies initiated in Category I. Category III encompassed study of power spectrum, carrier-to-interference effects, correlation of short and long paths, and further tests of multiplexer performance. Evaluation of a degradation monitor and baseband impulse noise were addressed under Category IV. At the completion of Category I testing, test priorities were reevaluated and Category III and IV were eliminated. Category II was modified to include expanded noise testing and evaluation of the degradation monitor.

1.3 General Test Objectives. The purpose of these tests performed on the DEB CONUS link is to establish a data base and performance assessment of a similar microwave system in advance of the final implementation of DEB Stage 1. These tests measure the key parameters of partial response transmission over a microwave line-of-sight link. Comparison of actual measurements of RSL availability to mathematical predictions establish the validity of those models, and confidence in the reliability of similar path predictions. Measurement of fade depths, rates, and durations forms a basis to calculate space diversity availability, expected BER availability, and correlation of error occurrence. BER vs RSL computations are the basic mode of system performance assessment. Baseband repeater performance indicates the feasibility of operating long links without the regeneration of data at each terminal. Multiplexer assessment identifies possible sources of error generation and can provide a valid indication of system quality before errors occur.

1.4 Summary of Findings. Long term results (over nine months) show a close correlation of measured RSL performance and predicted RSL performance. Previously reported short term data was apparently for the worst performance period. The number of fades recorded for one direction of transmission differed significantly from those recorded for the opposite direction of transmission on the long link. Space diversity operation resulted in improved performance. The average bit error rate at MMT and MTL sites was 1.11×10^{-11} and 2×10^{-11} respectively. After eight links of repeaters without data regeneration a BER of 1.85×10^{-8} was measured, but the final terminal fade margin of 10 dB

indicates a low availability for this performance. Multiplexer violations occurred when errors did not occur, and as violations increased, errors occurred, but without a precise correspondence. The Baseband Degradation Monitor (BDM) achieves its goal of providing an analog indication of link degradation of a digital baseband for a single link. The use of the BDM to monitor a multi-hop link is questionable. Cross-polarized transmission maintained a mean isolation of 24 dB. The NPR test procedure in the technical manual for the AN/FRC-162 is incorrect and should be eliminated. The specified value of 55 dB cannot be achieved at the baseband loading of +2.5 dBm.

2. GENERAL

2.1 Description of Equipment.

2.1.1 The primary equipment used in this test included 10 T1-4000 multiplexers, six AN/FRC-162 radio systems, and two AN/FRC-165 radio systems.

2.1.2 The T1-4000 is a time division multiplexer (TDM) that accepts eight individual T1 lines, each at a nominal rate of 1.544 Mb/s. The multiplexer uses bit stuffing to cause all lines to attain a common rate, and low pass filters the resultant nonreturn to zero (NRZ) data stream to produce an analog partial response signal. Data is recovered in the receiver by passing the partial response waveform through amplitude slicers, and the resulting square waves from the high level and low level slicers are sent to an NRZ converter. The multiplexer uses a shift register scrambler to randomize the bit stream, which prevents an energy concentration at discrete frequencies in the transmitted RF spectrum.

2.1.3 The AN/FRC-162 is a one watt, frequency modulated radio system that operates in the 8 GHz band. The radio contains an on-line transmitter and receiver, a hot standby transmitter, and an errorless baseband switched diversity receiver. The baseband has been designed to accept an analog partial response signal with a bandwidth of 6.3 MHz. The service channel and supervisory channels are inserted in the baseband at 8.1 and 8.5 MHz. The output radio frequency (RF) spectrum is confined to a 45 MHz bandwidth by a 45 MHz bandpass filter and a modulation index of 0.5.

2.1.4 A traveling wave tube (TWT) final amplifier is added to the AN/FRC-162 to produce a five watt transmitter. In this configuration, the radio is identified as the AN/FRC-165.

2.2 Summary of AN/FRC-162 Test Results.

2.2.1 The AN/FRC-162 radio system is the heart of the DEB Stage 1 equipment and therefore of primary interest. For a thorough discussion of

testing and engineering analysis, the reader should refer to Digital Transmission Evaluation Project, AN/FRC-162 Test, Final Report, CCC-CED-76-DTEP-011, published May 1976.

2.2.2 The BER vs RSL curve showed a performance variation among four radio combinations of 2.5 dB, which was partially dependent on alignment of the transmitter-receiver combination and differences in noise figure. The best combination yielded a curve displaced 3.5 dB from the referenced theoretical limits. These relationships are depicted in Figure 6. Resistance to co-channel interference varied, with a 2 dB degradation apparent at a carrier-to-interference ratio (C/I) equal to 18 dB and 8 dB degradation apparent at C/I equal to 12 dB. The worst interference effects under conditions of swept frequency interference occurred at 6.3 MHz from the carrier frequency. If FCC out-of-band limitations had been required, the spectrum would not have met the 14 MHz mask. The first shoulder would require up to 10 dB additional attenuation for compliance. The 99% power bandwidth was 12 MHz. The errorless receiver diversity switch operated error free under normal conditions at high and low RSL's.

2.2.3 Availabilities of various BER's over the CTA to Site Sibyl microwave link are plotted in Figure 7. This display indicates degradation due to the path and operational considerations not accounted for in back-to-back tests.

2.3 Test Methodology and Limitations.

2.3.1 The procedures in testing equipment and systems followed a published test plan adapted from standard practices as established in Technical Evaluation Line of Site and Troposcatter Links, DCS Quality Assurance Program, DCAC 310-70-57, Supplement 1, October 1974. Details of specific methodology are discussed under "Procedure" in each test section.

2.3.2 Automatic gain control (AGC) voltages in the receivers under test were calibrated to actual RSL values, thereby permitting convenient monitoring of the RSL through AGC variation. This calibration was performed weekly. All BER measurements used a pseudo-random pattern in excess of 1,000,000 bits (2^{20}) in length. All data collected was used in analysis except those portions obviously not representative of typical performance and clearly correlated to equipment or procedural failures.

2.3.3 In February 1977 an automated data collection system was installed for the long path propagation studies. This system, discussed in Appendix C, provided extended capabilities for analysis of fade characteristics.

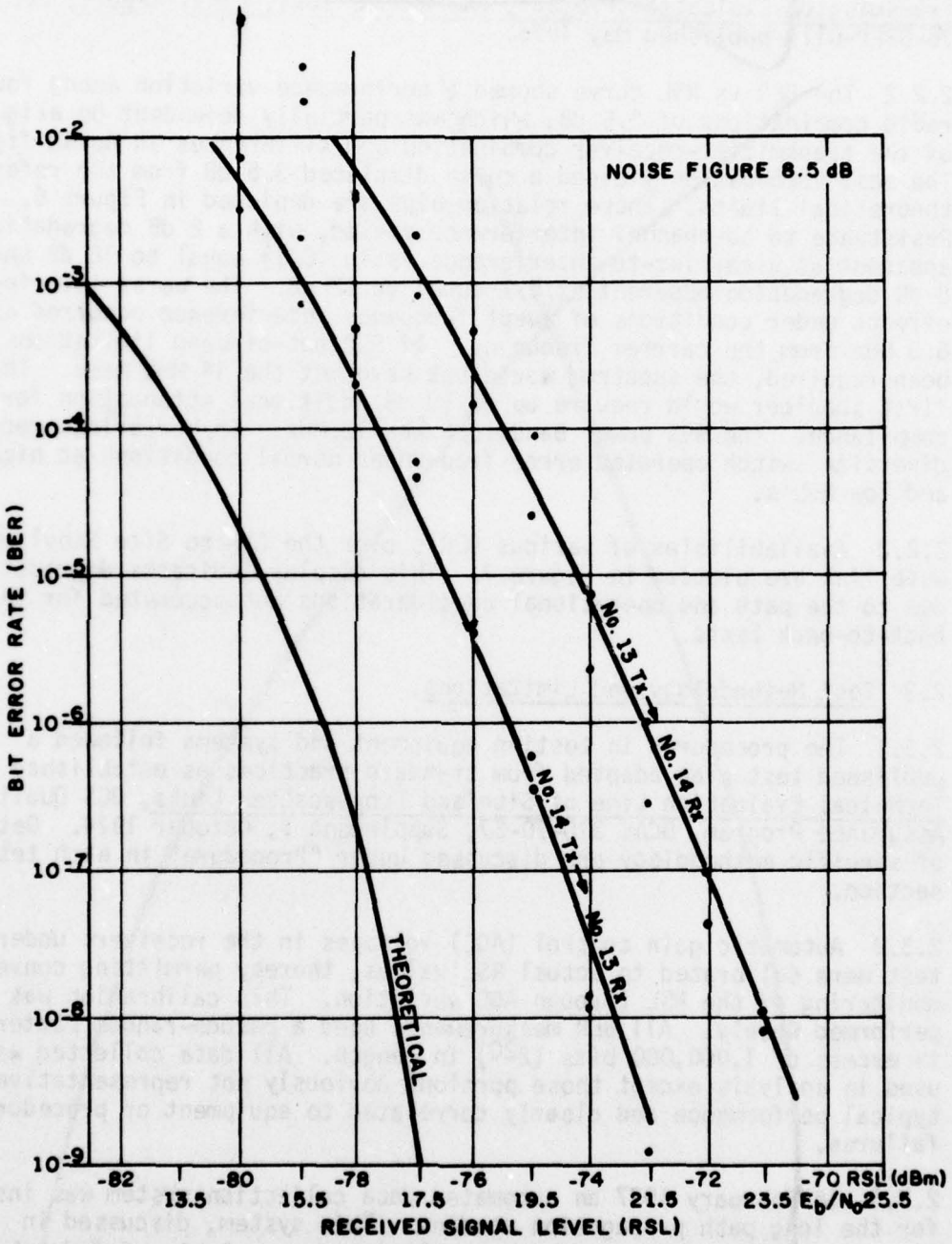

AN/FRC 162

Figure 6 Bit Error Rate vs Received Signal Level Characteristic Curves

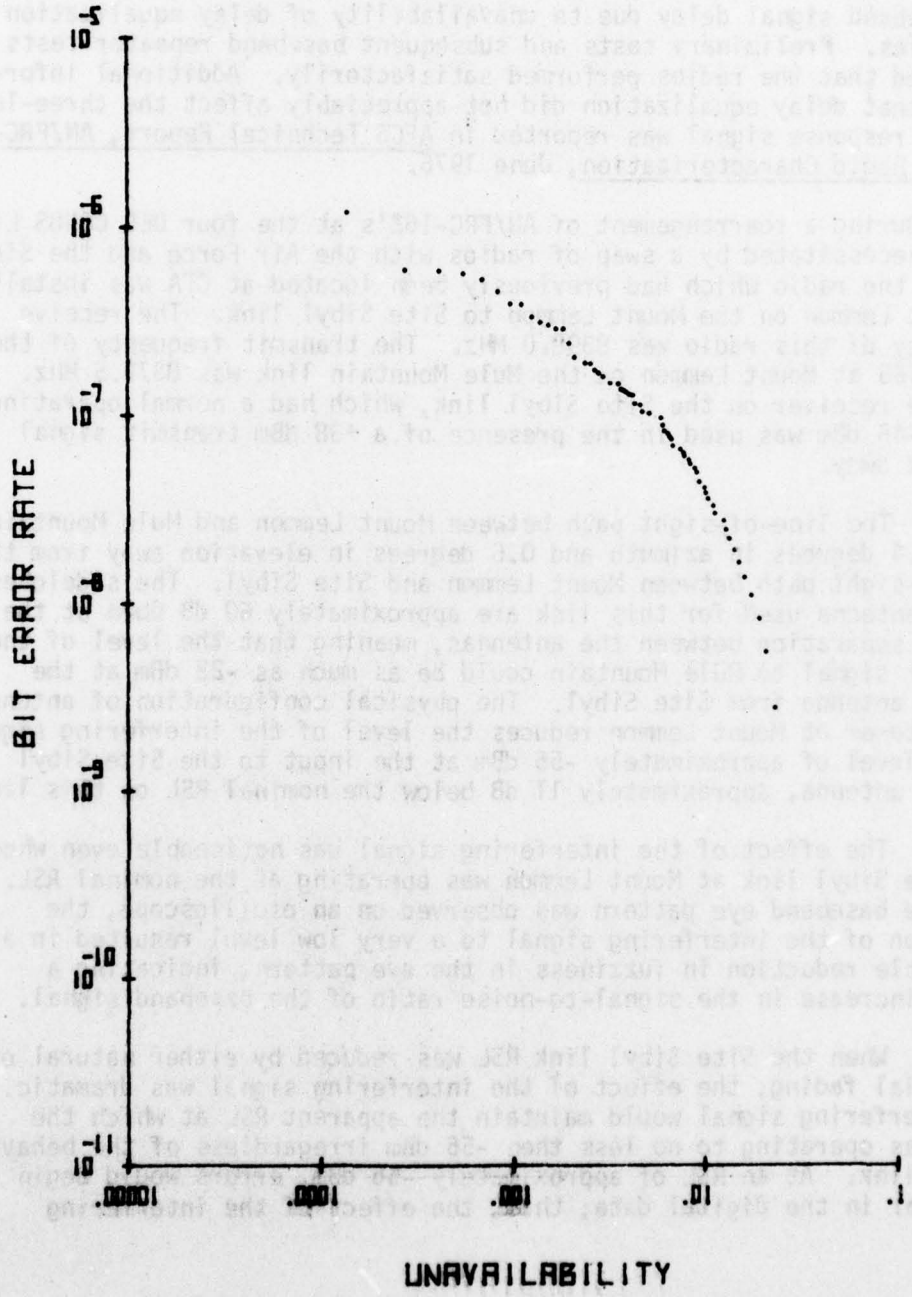

Figure 7. AN/FRC 162 Bit Error Rate vs Unavailability

2.4 Unscheduled Test Observations.

2.4.1 During the installation of equipment establishing the four terminals used in this project, the AN/FRC-162 radios were not equalized for baseband signal delay due to unavailability of delay equalization submodules. Preliminary tests and subsequent baseband repeater tests indicated that the radios performed satisfactorily. Additional information that delay equalization did not appreciably affect the three-level partial response signal was reported in AFCS Technical Report, AN/FRC-162 Digital Radio Characterization, June 1976.

2.4.2 During a rearrangement of AN/FRC-162's at the four DEB CONUS Link sites, necessitated by a swap of radios with the Air Force and the Signal School, the radio which had previously been located at CTA was installed at Mount Lemmon on the Mount Lemmon to Site Sibyl link. The receive frequency of this radio was 8398.0 MHz. The transmit frequency of the AN/FRC-165 at Mount Lemmon on the Mule Mountain link was 8379.5 MHz. Thus the receiver on the Site Sibyl link, which had a normal operating RSL of -45 dBm was used in the presence of a +38 dBm transmit signal 19.5 MHz away.

2.4.2.1 The line-of-sight path between Mount Lemmon and Mule Mountain lies 11.4 degrees in azimuth and 0.6 degrees in elevation away from the line-of-sight path between Mount Lemmon and Site Sibyl. The sidelobes of the antenna used for this link are approximately 60 dB down at the azimuth separation between the antennas, meaning that the level of the transmit signal to Mule Mountain could be as much as -22 dBm at the receive antenna from Site Sibyl. The physical configuration of antennas on the tower at Mount Lemmon reduces the level of the interfering signal to the level of approximately -56 dBm at the input to the Site Sibyl receive antenna, approximately 11 dB below the nominal RSL on this link.

2.4.2.2 The effect of the interfering signal was noticeable even when the Site Sibyl link at Mount Lemmon was operating at the nominal RSL. When the baseband eye pattern was observed on an oscilloscope, the reduction of the interfering signal to a very low level resulted in a noticeable reduction in fuzziness in the eye pattern, indicating a marked increase in the signal-to-noise ratio of the baseband signal.

2.4.2.3 When the Site Sibyl link RSL was reduced by either natural or artificial fading, the effect of the interfering signal was dramatic. The interfering signal would maintain the apparent RSL at which the radio was operating to no less then -56 dBm irregardless of the behavior of the link. At an RSL of approximately -56 dBm, errors would begin to appear in the digital data; thus, the effect of the interfering

signal was to decrease the fade margin on the Mount Lemmon to Site Sibyl link from 35 dB to 11 dB.

2.4.3 Waveguide connectors manufactured by Prodelin were found to be deficient in matching rigid to semi-rigid waveguides. After tuning, this connector interface resulted in a 16-22 dB return loss over a frequency band of $f_0 \pm 10$ MHz. Military Standard 188-313, Subsystem Design and Engineering Standards and Equipment Technical Design Standards for Long-Haul Communication Traversing Microwave LOS Radio and Tropospheric Scatter Radio; paragraph 5.11.2.2 states a requirement for a minimum return loss of 26 dB. Similar connectors made by Andrew Corporation interfaced waveguides with a resulting return loss of 30 dB over the same frequency range. The difference in performance may be explained by the difference in design. The Andrew Corporation device uses five tuning screws while Prodelin uses three. While Prodelin may manufacture a connector that is electrically equivalent to the Andrew device, the connector procured for these tests was not suitable.

2.4.4 The delay equalization measurement described in the technical manual for the AN/FRC-162 results in an oscilloscope waveform display of the classic delay envelope revealing the amount of slope and tilt of the radio baseband, which in turn is an indicator of the proper alignment of the baseband. During the setup of the radios on the various links, particularly at Site Sibyl and Mule Mountain, a large sinusoidal-type oscillation was found in this waveform. The amplitude of this oscillation was greater than could be equalized using the equalizer kits supplied with the radios. It was originally assumed that this oscillation was related to the grounding problems at these sites.

2.4.5 During checks of a degradation problem on the Site Sibyl link antenna at Mount Lemmon the real cause of the oscillation was discovered. A delay equalization measurement on this link had revealed an oscillation in the waveform. Checks of the waveguide to the antenna revealed a bent section, which was removed. A delay equalization measurement taken after the waveguide repair had been completed revealed that the oscillation had disappeared. Apparently, the delay equalization test set acts like a frequency domain reflectometer in sensing waveguide and antenna imperfections.

3. DETAILS OF TESTING

3.1 Received Signal Levels: Predicted vs Actual.

3.1.1 Objective. The purpose of this test is to compare actual measurements of RSL availability to mathematical predictions. This comparison yields information concerning the reliability of the predictions of other

similar microwave paths.

3.1.2 Procedure.

3.1.2.1 A path profile was plotted and system performance computed using techniques based on National Bureau of Standards Transmission Loss Predictions for Tropospheric Communication Circuits, Technical Note Number 101. Appendices A and B provide technical information and actual path profiles, respectively.

3.1.2.2 The AGC voltages were recorded by continual strip chart recording, and at intervals by a digital printer as illustrated in Figure 8. Instantaneous values were initially recorded at approximately one, two, or five minute intervals and a comparison of results led to the determination to use the one minute samples. The one minute samples were incorporated into the automated data collection system format (see Appendix C) to provide continuity throughout the test period. Use of the digital printer was discontinued after initial checkout of the automated system.

3.1.2.3 Samples were taken at the Mule Mountain (MMT) site and the Mount Lemmon (MTL) site from July 15, 1976 to April 30, 1977. During this period data was produced for approximately 220-24 hour days at MMT and 190-24 hour days at MTL.

3.1.3 Results and Analysis.

3.1.3.1 At the MMT site 322,458 samples were taken and at the MTL site 156,583 samples were taken. Figure 9 shows the availability of RSL for each end of the 82-mile link. Availability calculation is based upon the instantaneous samples taken every minute. Of these samples 99.98+/% were above -65 dBm, the point at which receiver switching occurs. These samples are for the "B" receiver only and diversity improvement is not considered.

3.1.3.2 The 50% confidence and 95% confidence predicted hourly medians are plotted in Figure 10. The availability of the instantaneous samples closely follows this curve until the 99.9% point. At this point, divergence is expected. Since the number of samples below -65 dBm is much less than a sixteenth of the total number of samples, the hourly median of the samples would not reflect the low RSL's.

3.1.3.3 The hourly medians were obtained for the period during which the automatic data collection system was operational and are shown in Figure 10. The plot for the MTL site is slightly below predicted level for 50% confidence while the plot for the MMT site is slightly below the 95% confidence level. The results are not identical at each end of the link.

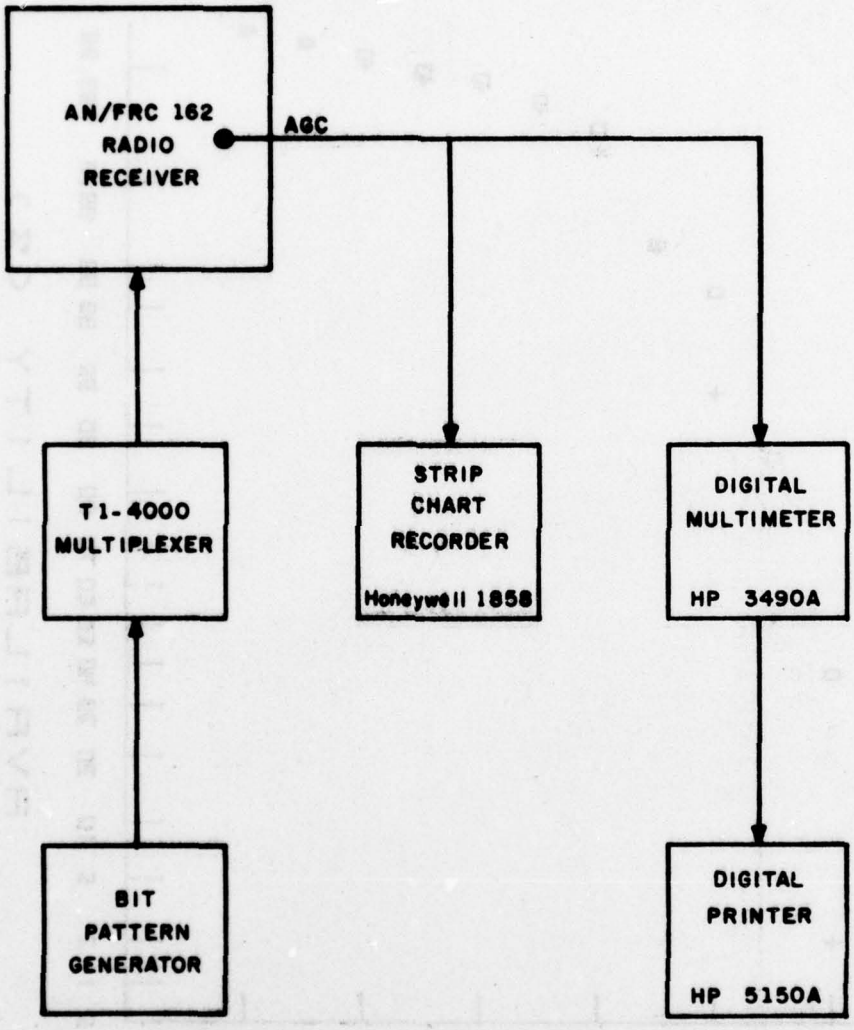

Figure 8. Test Configuration for Received Signal Level Measurement

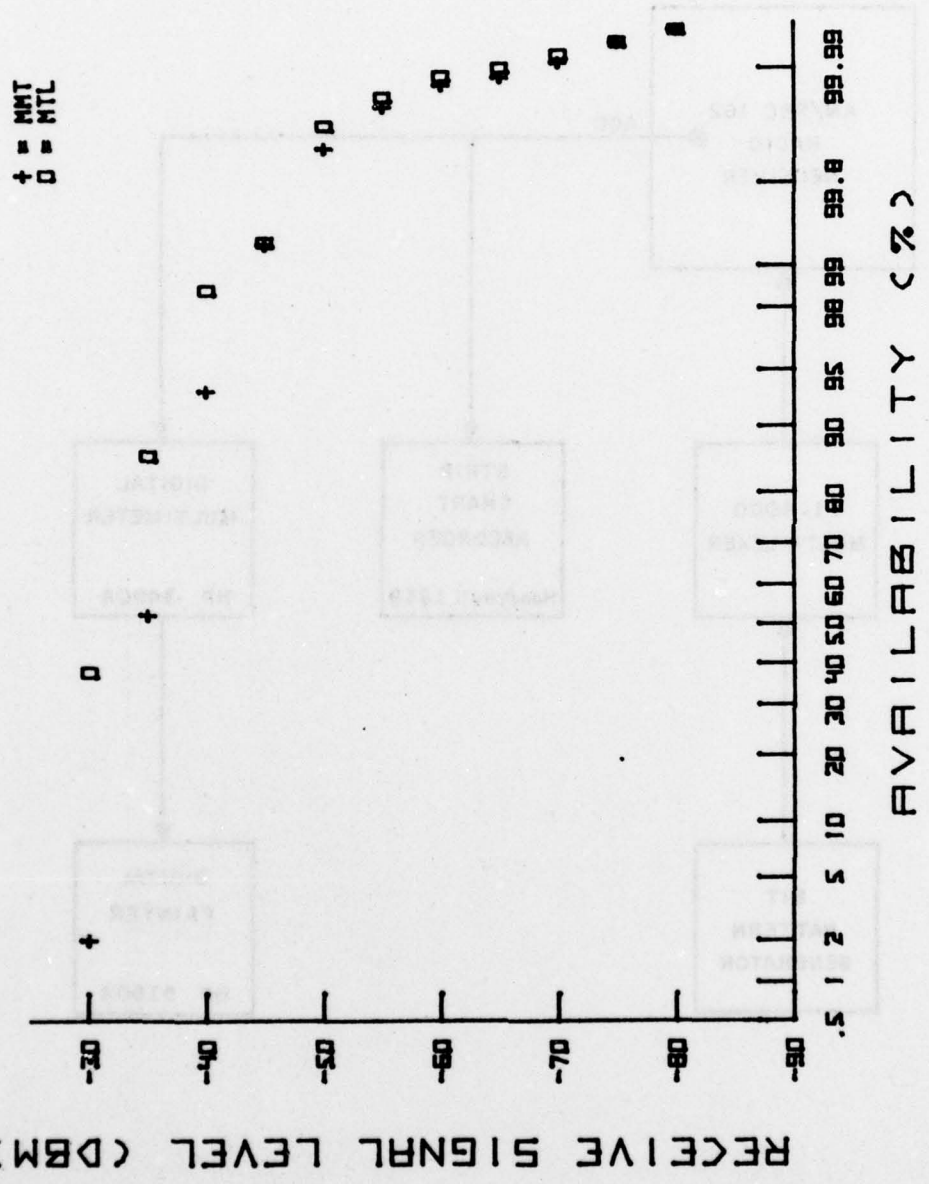

Figure 9. Sample RSL Availability

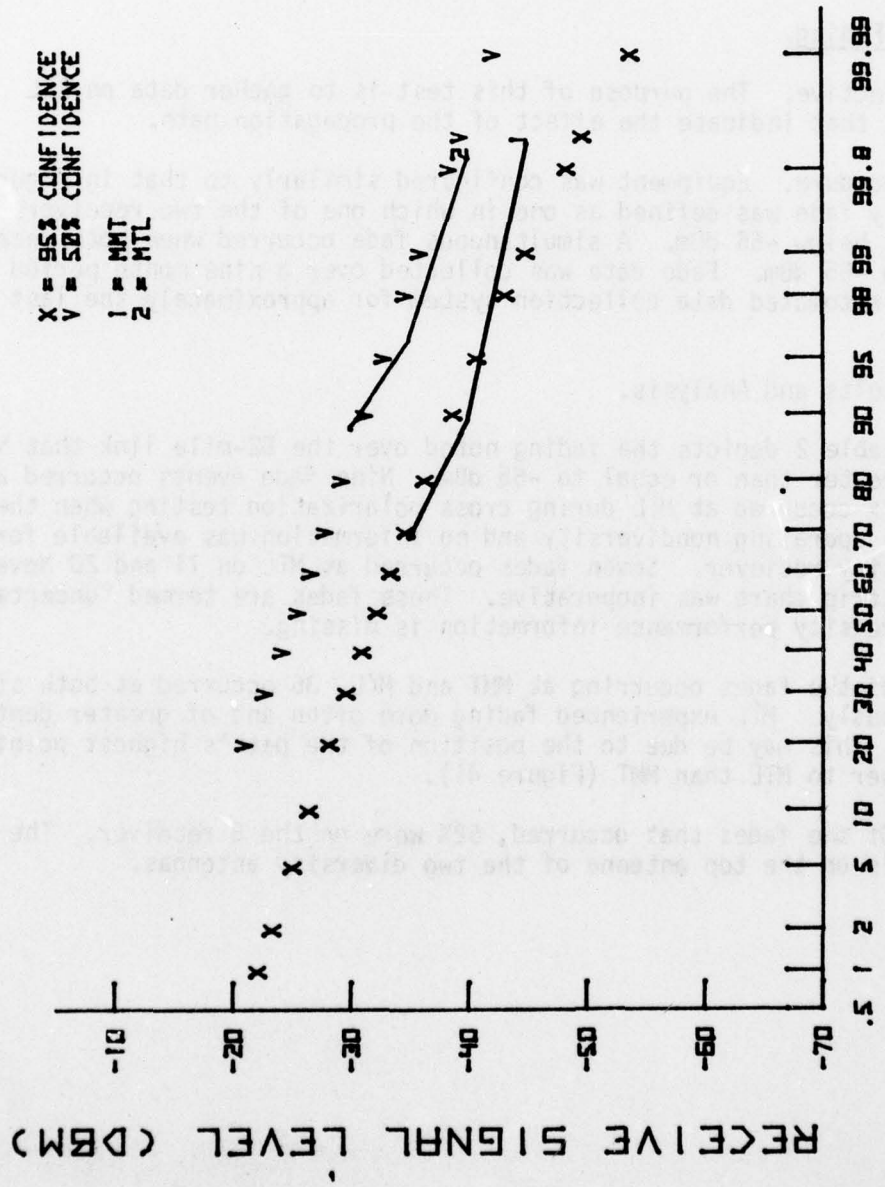

Figure 10.. Predicted vs Actual Received Signal Level Relationship

3.1.3.4 The predictions were based on a nondiversity system. The diversity improvement is not a factor when dealing with hourly medians. Also provided was an extrapolation of the predictions that showed a time availability for a diversity system at an RSL of -69 dBm of 99.99987 and for a nondiveristy system at an RSL of -69 dBm of 99.95894. The extrapolation is based upon fades with a Rayleigh distribution around the 50% confidence level.

3.2 Path Fading.

3.2.1 Objective. The purpose of this test is to gather data on RSL variations that indicate the effect of the propagation path.

3.2.2 Procedure. Equipment was configured similarly to that in Figure 8. A diversity fade was defined as one in which one of the two receivers had an RSL below -65 dBm. A simultaneous fade occurred when both receivers were below -65 dBm. Fade data was collected over a nine month period using the automated data collection system for approximately the last two months.

3.2.3 Results and Analysis.

3.2.3.1 Table 2 depicts the fading noted over the 82-mile link that had a depth greater than or equal to -65 dBm. Nine fade events occurred at MMT and six occurred at MTL during cross polarization testing when the system was operating nondiversity and no information was available for the diversity reciever. Seven fades occurred at MTL on 11 and 20 November when the strip chart was inoperative. These fades are termed "uncertain", as the diversity performance information is missing.

3.2.3.2 Of the fades occurring at MMT and MTL, 36 occurred at both sites simultaneously. MTL experienced fading more often and of greater depth than MMT. This may be due to the position of the path's highest point being closer to MTL than MMT (Figure 41).

3.2.3.3 Of the fades that occurred, 62% were on the B receiver. The B receiver is on the top antenna of the two diversity antennas.

Table 2. Long Link Fades

TYPE FADE	Number of Fades at Receiver MMT	MTL
Diversity	128	148
Simultaneous	2	8
Nondiveristy	9	6
Uncertain	0	6
Receiver Outages		
A RCVR	49 (35%)	73 (42%)
B RCVR	92 (65%)	103 (58%)

3.3 Bit Error Rate Measurements.

3.3.1 Objective. The purpose of this test is to record the number of errors occurring over a period of time in order to compute a BER.

3.3.2 Procedure. A bit pattern generator was connected to a T1 input of the T1-4000. A random bit pattern was connected to a second T1 input and looped six times in order to fully load the multiplexer. Errors were counted on a bit error test set, while RSL's were monitored as previously depicted in Figure 8.

3.3.3 Results and Analysis.

3.3.3.1 Errors were counted at the MMT and MTL sites over the period 1 September 1976 to 30 April 1977. There were a total of 197,580 samples and 195,703 samples taken at MMT and MTL respectively. This represented 78% and 79% of the days in the period. RSL distributions over the same period are given in section 3.2.

3.3.3.2 Table 3 is a description of the error distribution for MMT. Of the 197,580 samples, six were dropouts caused by loss of synchronization. The average BER was 1.1×10^{-11}.

3.3.3.3 Table 4 describes the error distribution for MTL. Of the 195,703 samples, 10 were overflows. The average BER was 2.1×10^{-11}.

TABLE 3. MET ERROR DISTRIBUTION

ERROR COUNT	FREQUENCY	SAMPLE BER	AVAILABILITY(%)
0	197434	0.00E-00	99.929
1	103	1.33E-09	99.981
2	7	2.66E-09	99.984
4	5	5.31E-09	99.987
5	4	6.64E-09	99.989
7	2	9.29E-09	99.990
10	1	1.33E-08	99.990
11	1	1.46E-08	99.991
14	1	1.86E-08	99.991
16	2	2.12E-08	99.992
17	1	2.26E-08	99.992
21	2	2.79E-08	99.994
22	1	2.92E-08	99.994
25	1	3.19E-08	99.995
27	1	3.58E-08	99.995
29	1	3.85E-08	99.996
36	1	4.78E-08	99.996
45	1	5.97E-08	99.997
59	1	7.83E-08	99.997
81	1	1.08E-07	99.998
152	1	2.02E-07	99.998
324	1	4.30E-07	99.999
547	1	7.26E-07	100.000

NUMBER OF SAMPLES = 197574
AVERAGE BER = 1.1041E-11

TABLE 4. MTL ERROR DISTRIBUTION

ERROR COUNT	FREQUENCY	SAMPLE BA	AVAILABILITY (%)
0	195607	0.00E 00	99.956
1	41	1.33E-09	99.977
2	7	2.66E-09	99.980
3	2	3.98E-09	99.981
4	1	5.31E-09	99.982
5	3	6.64E-09	99.983
6	1	7.97E-09	99.984
7	1	9.29E-09	99.984
8	1	1.06E-08	99.985
10	1	1.33E-08	99.985
13	1	1.73E-08	99.986
14	1	1.86E-08	99.986
18	2	2.39E-08	99.987
21	1	2.79E-08	99.988
24	2	3.19E-08	99.989
26	2	3.45E-08	99.990
27	1	3.58E-08	99.990
29	2	3.85E-08	99.991
41	1	5.44E-08	99.992
42	1	5.58E-08	99.992
46	2	6.11E-08	99.992
51	1	6.77E-08	99.994
61	1	8.10E-08	99.994
72	1	9.56E-08	99.995
82	1	1.09E-07	99.995
83	1	1.10E-07	99.996
104	1	1.38E-07	99.996
111	1	1.47E-07	99.997
208	1	2.76E-07	99.997
213	1	2.83E-07	99.998
280	1	3.72E-07	99.998
505	1	6.71E-07	99.999
849	1	1.13E-06	100.000

NUMBER OF SAMPLES = 195693
AVERAGE BER = 2.1535E-11

3.4 Baseband Repeater Operation.

3.4.1 Objective. The purpose of this test is to study the degradation of signal quality as the signal is relayed from one terminal to another without regeneration of the data by multiplexers. Baseband frequency response, BER, and percent error free samples are reported to indicate this degradation.

3.4.2 Procedure. Figure 11 depicts the test configuration for baseband repeater operation. The test signal was repeated up to a maximum eight links, employing seven baseband repeaters. Figure 12 depicts the two route configurations used to attain this maximum.

3.4.3 Results and Analysis.

3.4.3.1 Figure 13 is a frequency response curve showing the baseband response for the eight-hop repeater operation. The frequency response can be stated as 370 Hz to 7.2 MHz +1, -3 dB. Table 5 lists the RSL's for a BER of 10^{-6} at each terminal of the eight-hop transmission link showing the elevation of required threshold.

3.4.3.2 Figure 14 shows four baseband frequency response curves. The illustration shows the small change in amplitude response as the number of hops was increased from one to four.

3.4.3.3 Figure 15 shows seven oscillographs of the three-level partial response eye pattern. The clarity and symmetry of these patterns is an indication of the signal quality at each succeeding repeater terminal. Degradation can be seen to accumulate and appears especially poor at Site Sibyl (4th terminal) where interference from another transmitter located at Mount Lemmon was a factor.

3.4.3.4 Figure 16 includes ten oscillographs of the baseband spectra. The 8.1 and 8.5 MHz subcarriers are evident as spikes in the spectrum. The shape of the spectrum and lack of distortion products is an indication of signal quality. The degradation as measured in other tests does not appear clearly in these oscillographs as the number of repeaters was increased. (NOTE: The slight drop in response evident at the low frequency portion of the spectra is due to test equipment limitations).

3.4.3.5 Table 5 lists the paths used on the eight-hop baseband repeater with the resultant RSL's recorded at the distant terminal. After eight hops of baseband repeaters, a BER of 1.85×10^{-8} was able to be maintained. This BER corresponded to an RSL of only -40 dBm and suggests a rather low availability. At the ninth terminal 98.8166% of the samples were error free.

Figure 11. Test Configuration for Baseband Repeater Operation

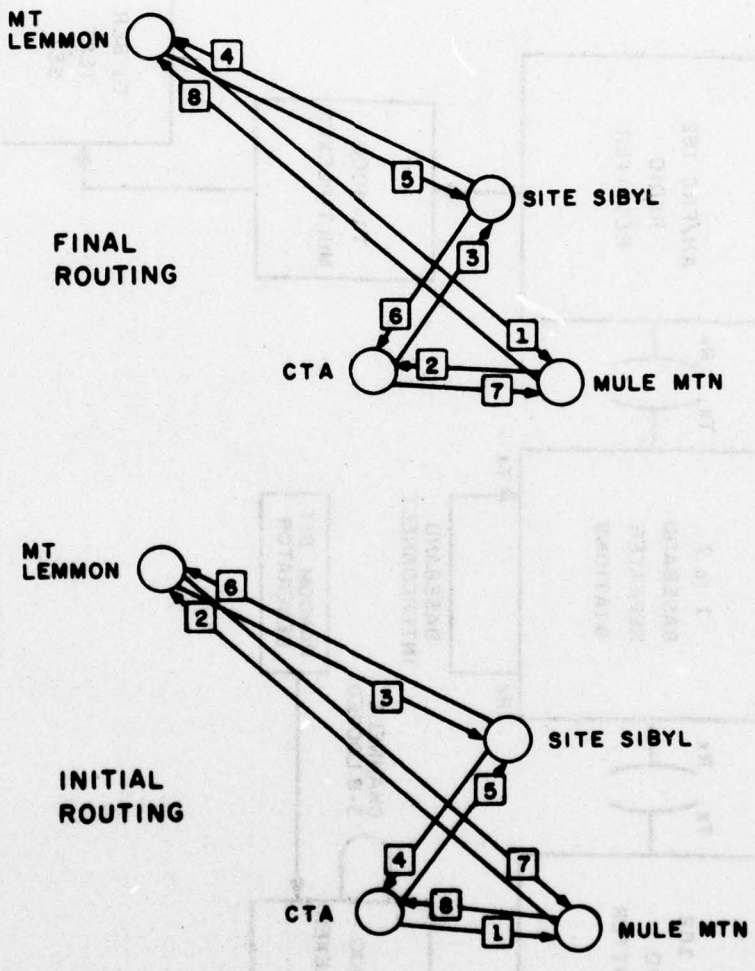

Figure 12. Eight-Hop Transmission Diagrams

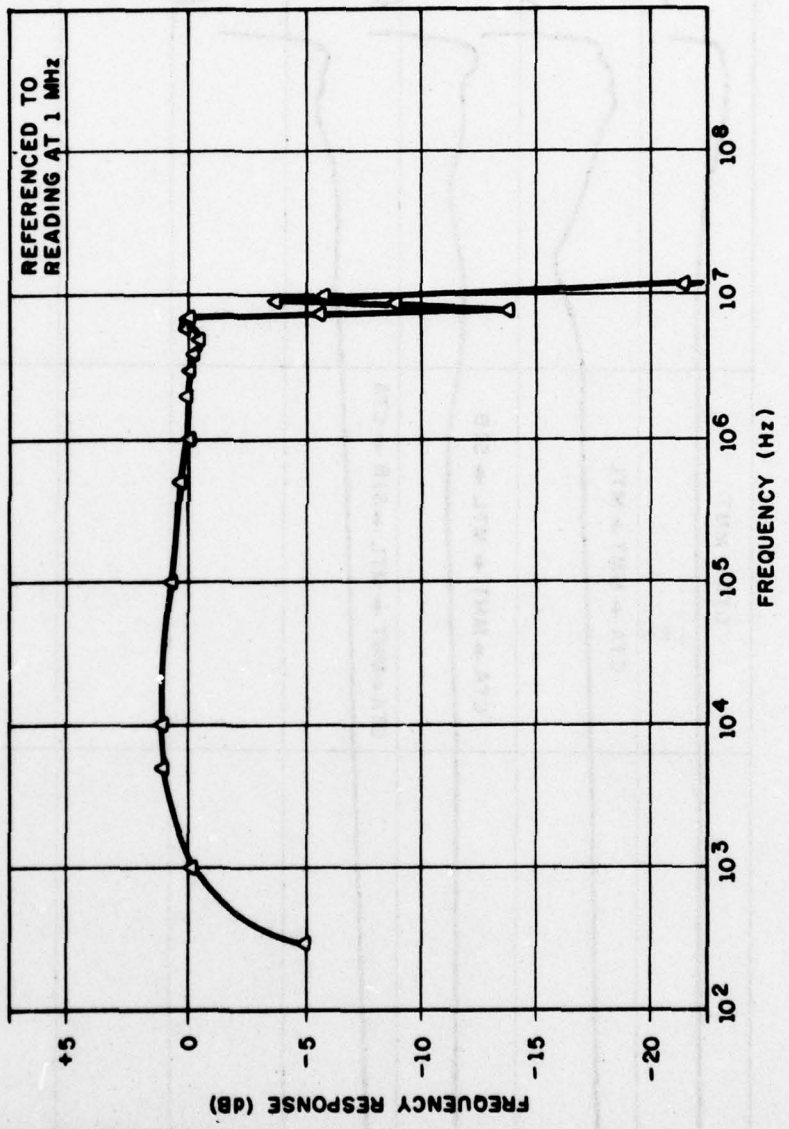

Figure 13. Baseband Frequency Response Characteristics for 8-Hop Transmission

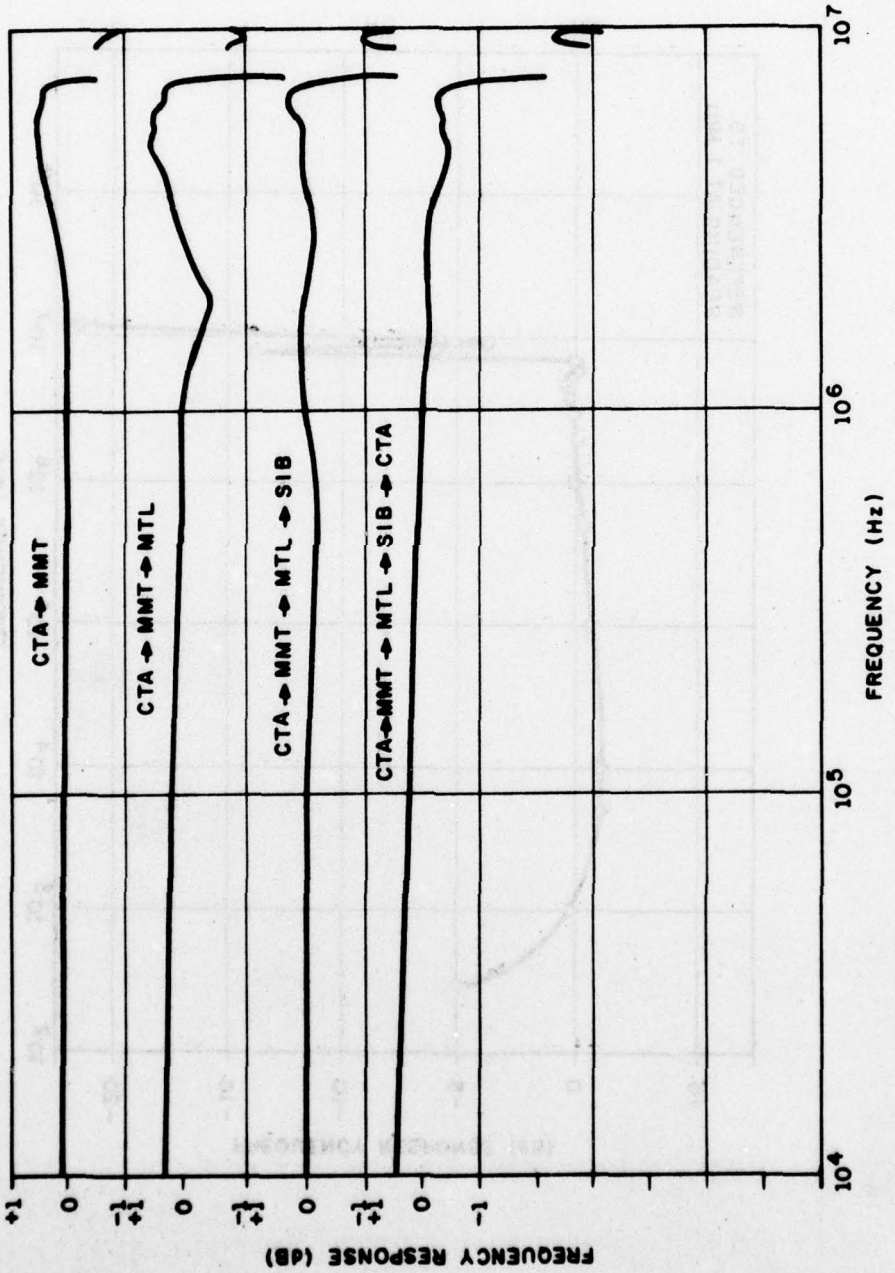

Figure 14. Baseband Frequency Response Characteristics for 1,2,3, and 4-Hop Transmissions

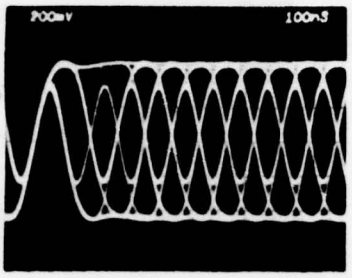

Reference

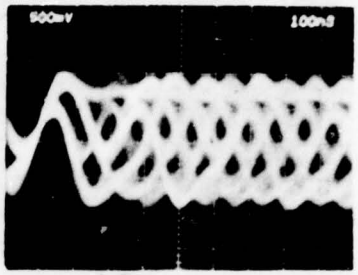

6th Terminal

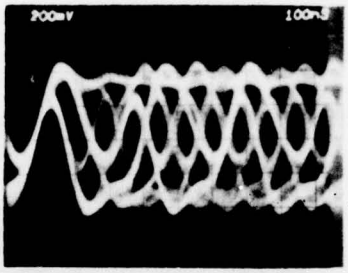

3rd Terminal

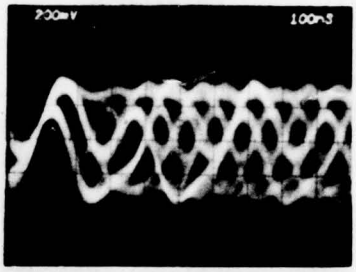

7th Terminal

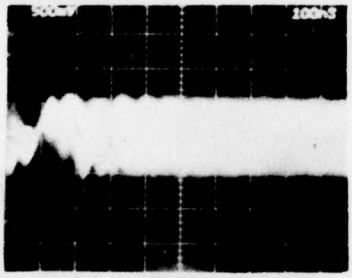

4th Terminal

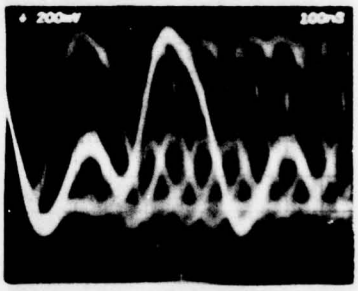

8th Terminal

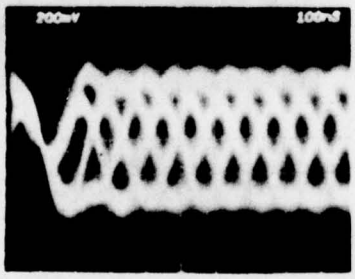

5th Terminal

Figure 15. Oscillographs of Eye Patterns for Baseband Repeater Operation

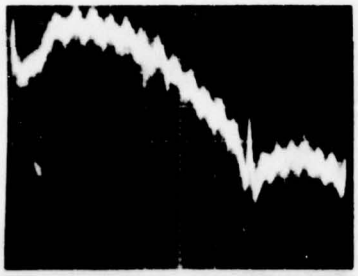

Multiplexer Output
Reference

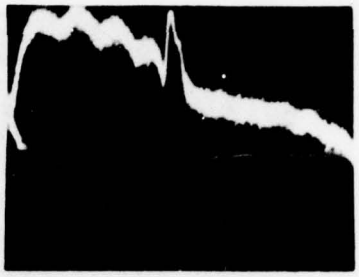

3rd Terminal

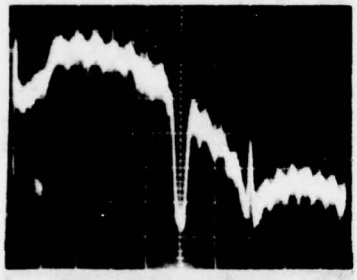

Radio Output
Reference

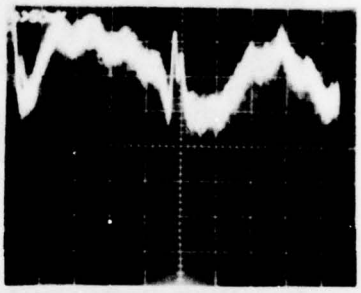

4th Terminal

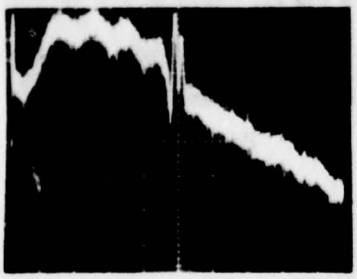

2nd Terminal

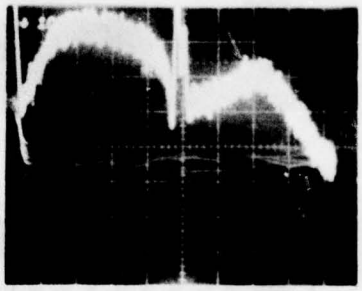

5th Terminal

Figure 16. Part I-Oscillographs of Sequential Baseband Spectra
(Repeater Operation)

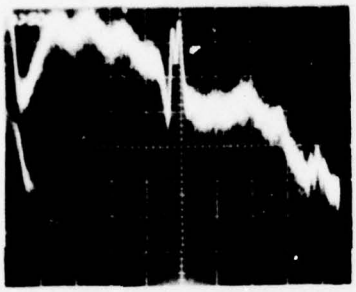

6th Terminal

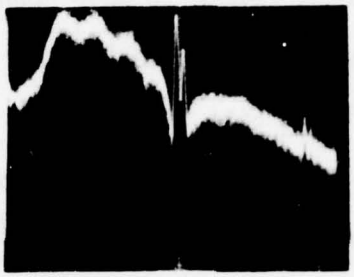

8th Terminal

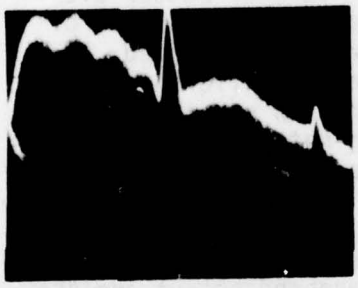

7th Terminal

9th Terminal

Figure 16. Part II-Oscillographs of Sequential Baseband Spectra (Repeater Operation)

Table 5. Baseband Repeater Performance

Path	Received Signal Level (dBm) to Give 1 x 10^{-6} BER
Mount Lemmon to Mule Mountain	-70.0
Mule Mountain to CTA	-67.0
CTA to Site Sibyl	-60.0
Site Sibyl to Mount Lemmon	-60.0
Mount Lemmon to Site Sibyl	-54.0
Site Sibyl to CTA	-68.0
CTA to Mule Mountain	Not measured
Mule Mountain to Mount Lemmon	-40.0

3.4.3.6 Results from this test confirmed that any combination of radios and multiplexers will support a BER of 5 x 10^{-9} or better after four relays of baseband repeaters. Although a gradual degradation of signal quality occurred as the number of repeaters was increased, the greatest variability of BER performance was caused by differing multiplexer sensitivities. Because of these differences in sensitivity, errors were recorded at one site when errors were not recorded at a subsequent site; that is, the second multiplex was better able to demultiplex the slightly degraded signal.

3.4.3.7 Results indicated that the system performance may be improved by using signal conditioning between the radio baseband output and the multiplexer input in order to remove out-of-band noise and the two subcarrier signals. Baseband repeaters created a system filter between two terminals. That is, at the repeater site the multiplexer used to monitor the baseband signal received perturbations caused by out-of-band noise, which was effectively removed by the band limiting characteristics of the transmitter for the next link. In this way the end terminal was not affected by the total out-of-band noise generated between the initial terminal and the intermediate repeater.

3.5 Multiplexer Performance.

3.5.1 Objective. The objective of this test is to record the number of major and minor multiplexer reframes. A major reframe indicates resynchronization of the entire data stream at the 12.5526 Mb/s level, and a minor reframe indicated resynchronization of a T1 data stream

within the total data stream. Reframes give indications of lowered signal quality and are an indication of performance degradation.

3.5.2 Procedure. A chart recorder was connected to the appropriate test points of two second-level multiplexers to record three-level partial response violations. Simultaneously, RSL's were recorded as described in section 3.1.2. Data for the two multiplexers was gathered as the RSL was varied by introducing attenuation in the transmitter waveguide.

3.5.3 Results and Analysis.

3.5.3.1 Violations did occur when errors did not occur. When errors and violations occurred simultaneously, there was no constant ratio between the numbers of violations and the number of errors. However, as the numbers increased in magnitude, the ratio of violations to errors diminished. In addition to errors causing reframes, these reframes created additional errors.

3.5.3.2 For multiplexer A, no major reframes occurred with an RSL of -81 dBm or higher. This RSL corresponded to a BER of 1×10^{-3}, and 172,000 violations/second. Similarly, no minor reframes occurred with an RSL of -75 dBm or higher. This RSL corresponded to a BER of 3×10^{-5} and 1812 violations/second. The maximum number of violations that occurred without an error was 214.

3.5.3.3 For multiplexer B, no major reframes occurred with an RSL of -78 dBm or higher. This RSL corresponded to a BER of 5×10^{-2}, and 240,000 violations/second. Similarly, no minor reframes occurred with an RSL of -74 dBm or higher. This RSL correlated with a BER of 4×10^{-4}, and 12,000 violations/second. The maximum number of violations that occurred without an error was 860.

3.6 Baseband Degradation Monitor.

3.6.1 Objective. This test provides data on the performance of the Baseband Degradation Monitor (BDM) developed by the Air Force Communications System (AFCS).

3.6.2 Procedure. The test configuration is shown in Figure 17. The link configuration was one to six hops as shown in Figure 12. The BDM was initially tested on a single link (CTA to MMT) to obtain the characteristic curve for the Receiver-Transmitter pairs. Then the links were reconfigured to obtain curves of BDM voltage as a function

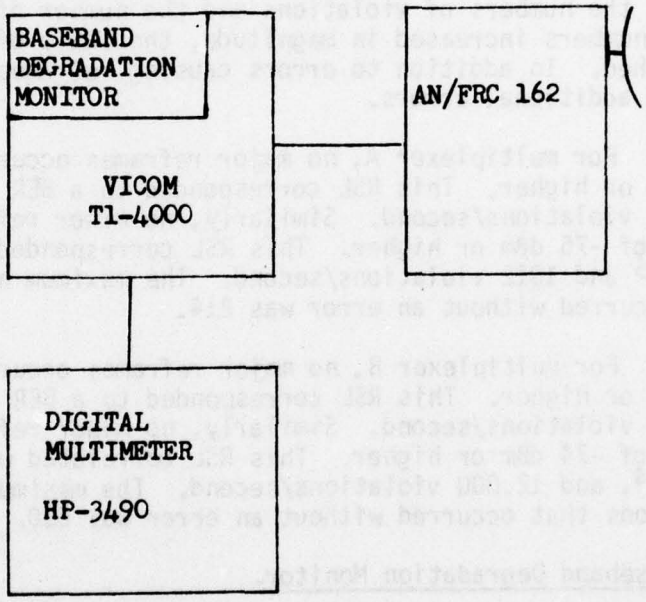

Figure 17. Test Configuration for Baseband Degradation Monitor

of RSL for a different number of baseband repeaters. The BDM slicer levels were adjusted after the six hop configuration was established. Then the transmitted signal was attenuated at each of the six repeater locations in turn. Finally, the same test was performed without realignment of the BDM each time a new repeater was added.

3.6.3 Results and Analysis.

3.6.3.1 The BDM is designed to provide a monitor of the signal-to-noise ratio (S/N) of a digital baseband. The circuit was designed to be implemented as a plug-in card for the VICOM T1-4000 multiplexer, which is the form in which it was evaluated at DTEP. The BDM provides a voltage output based upon the noise which is superimposed upon the "eye" voltage of the three-level partial response input to the T1-4000 multiplexer. The BDM has an adjustable voltage slicer level which is set at a particular voltage level (approximately 50 mv) which represents the ambient noise level on the three-level partial response signal. Additional noise on the "eye", created by a signal-to-noise ratio degradation will result in a larger voltage output from the BDM. A typical curve of the response of the BDM is shown in Figure 18.

3.6.3.2 The principle on which the BDM operates is shown in Figure 19. This figure represents the probability distributions of a "1" and a "0", assuming that the noise superimposed on the signal has a gaussian distribution. Setting the decision limits for a "1" to A and B, which is the normal procedure in the T1-4000, results in a very low error rate in normal circumstances and a voltage level which is essentially the level for "1". When the decision limits are moved out to C and D, which is done by setting the slicer levels on the BDM, a larger amount of the noise can be sensed. As the signal-to-noise ratio degrades, the normal slicer levels in the multiplexer maintain error-free performance down to very low signal-to-noise ratios. The broader slicer levels of the BDM allow this degradation to be sensed as an increase in voltage level. In effect, the BDM has created a "pseudo" error rate which is represented by the BDM voltage. Figure 20 is a typical curve of BDM voltage output for the Receiver-Transmitter pairs on the CTA to SIB link.

3.6.3.3 Figure 21 is the family of curves generated by attenuating in turn each site transmitter for a six hop configuration. This figure demonstrates that the use of the BDM as a monitor of a multi-hop link, with the BDM slicer adjusted for the complete link configuration, is not feasible. The degradation of one portion of the link can create a wide variation of BDM output voltage depending on which section of the overall link is degraded. For example, in Figure 21 a 1.5 volt signal from the BDM could mean that the Mount Lemmon to Site Sibyl link has degraded to -59 dBm or that the Mule Mountain to Mount Lemmon link has degraded to -72.5 dBm. The first case would be serious, but not critical; the second

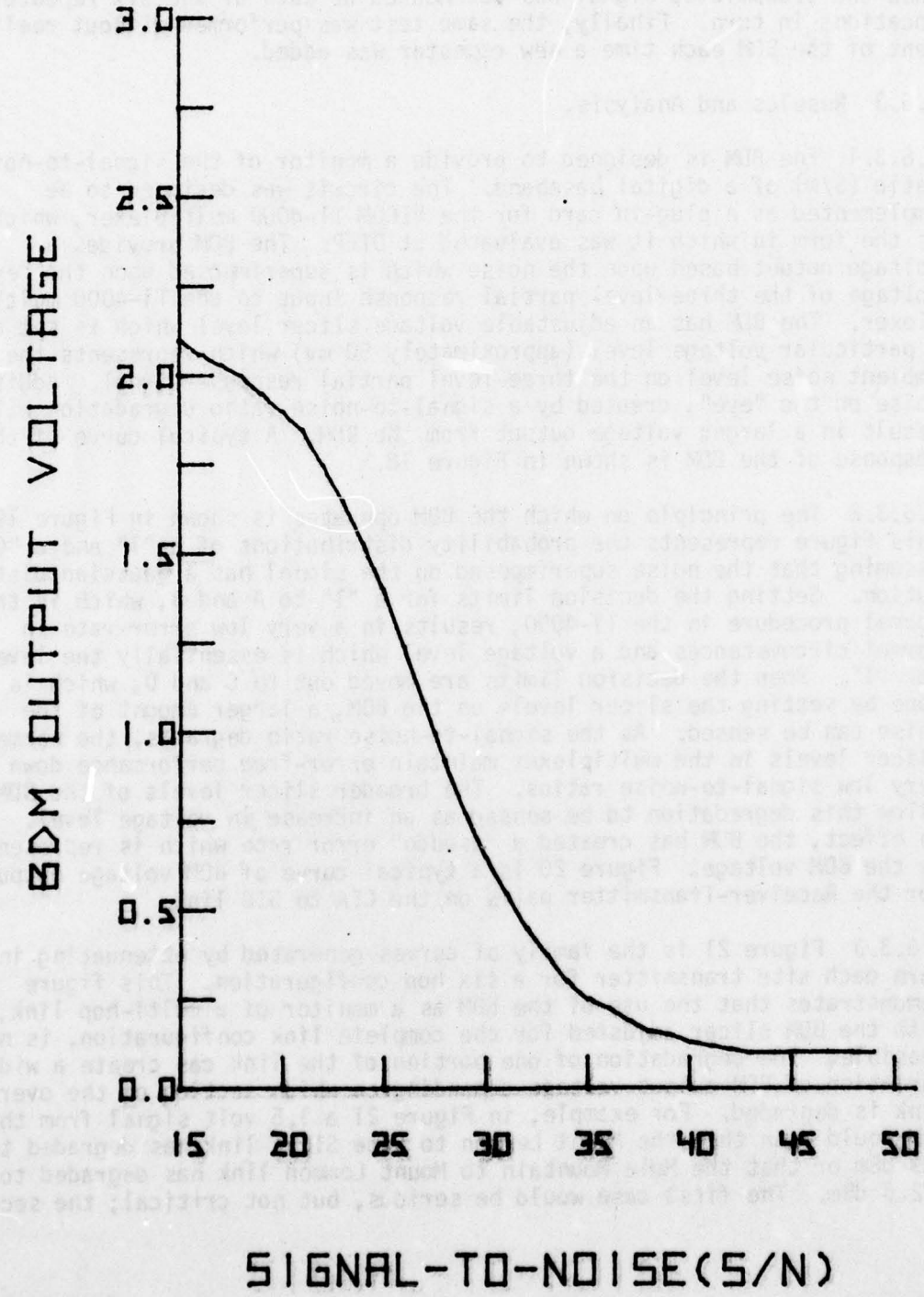

Figure 18. Typical Response Curve for BDM

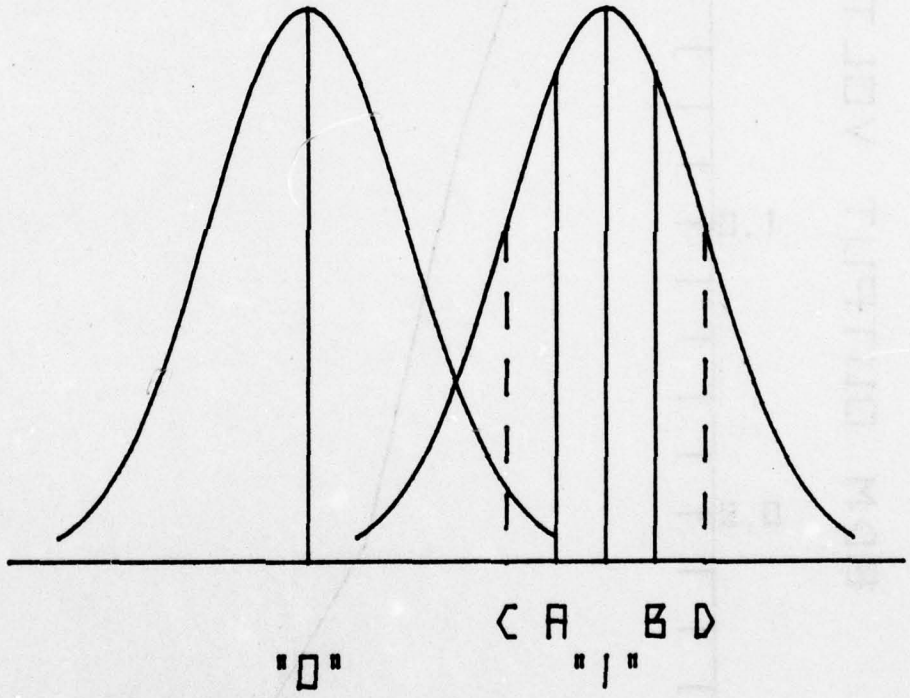

Figure 19. Normal Distribution for "0" and "1"

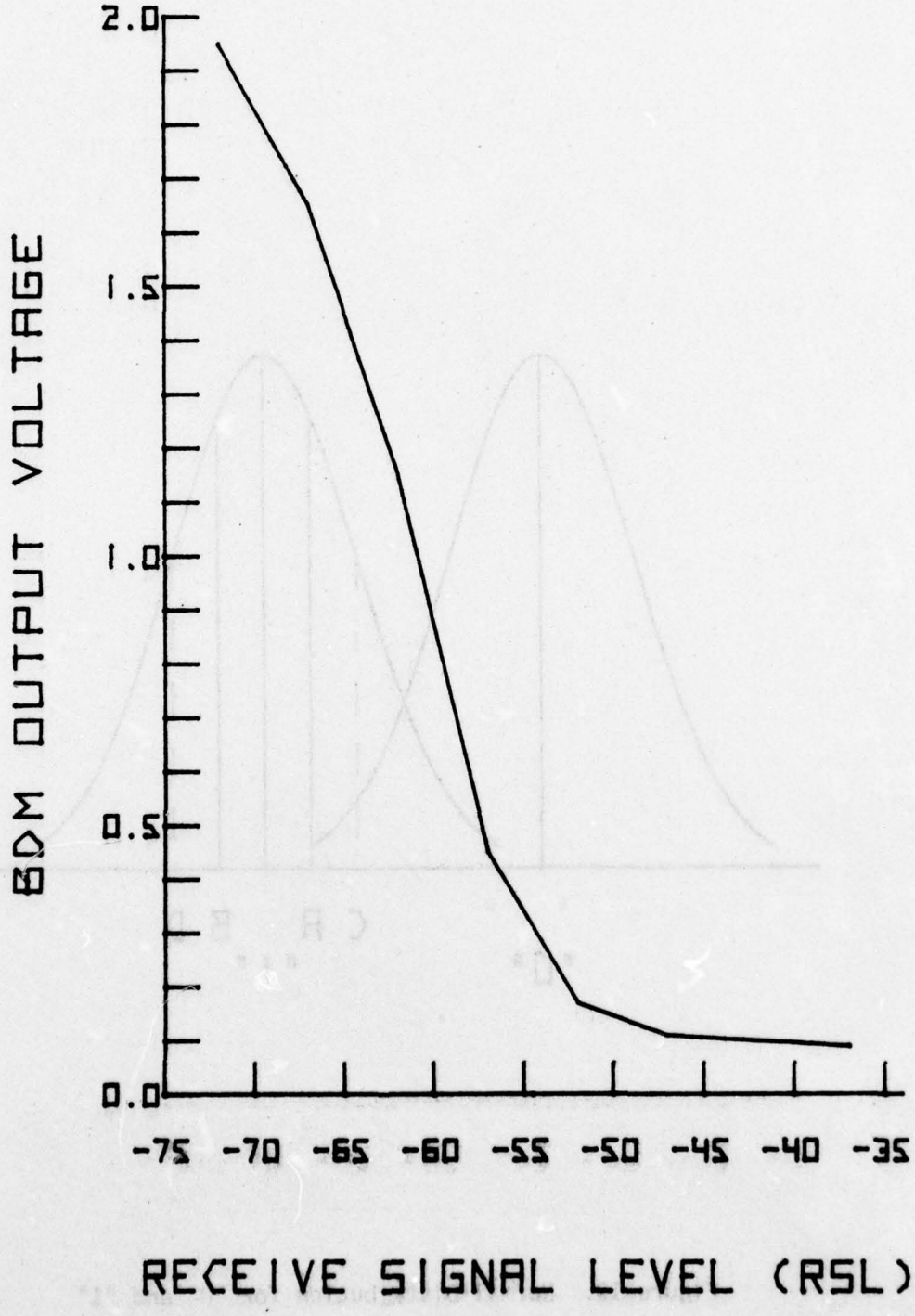

Figure 20. BDM Response for Six Hops

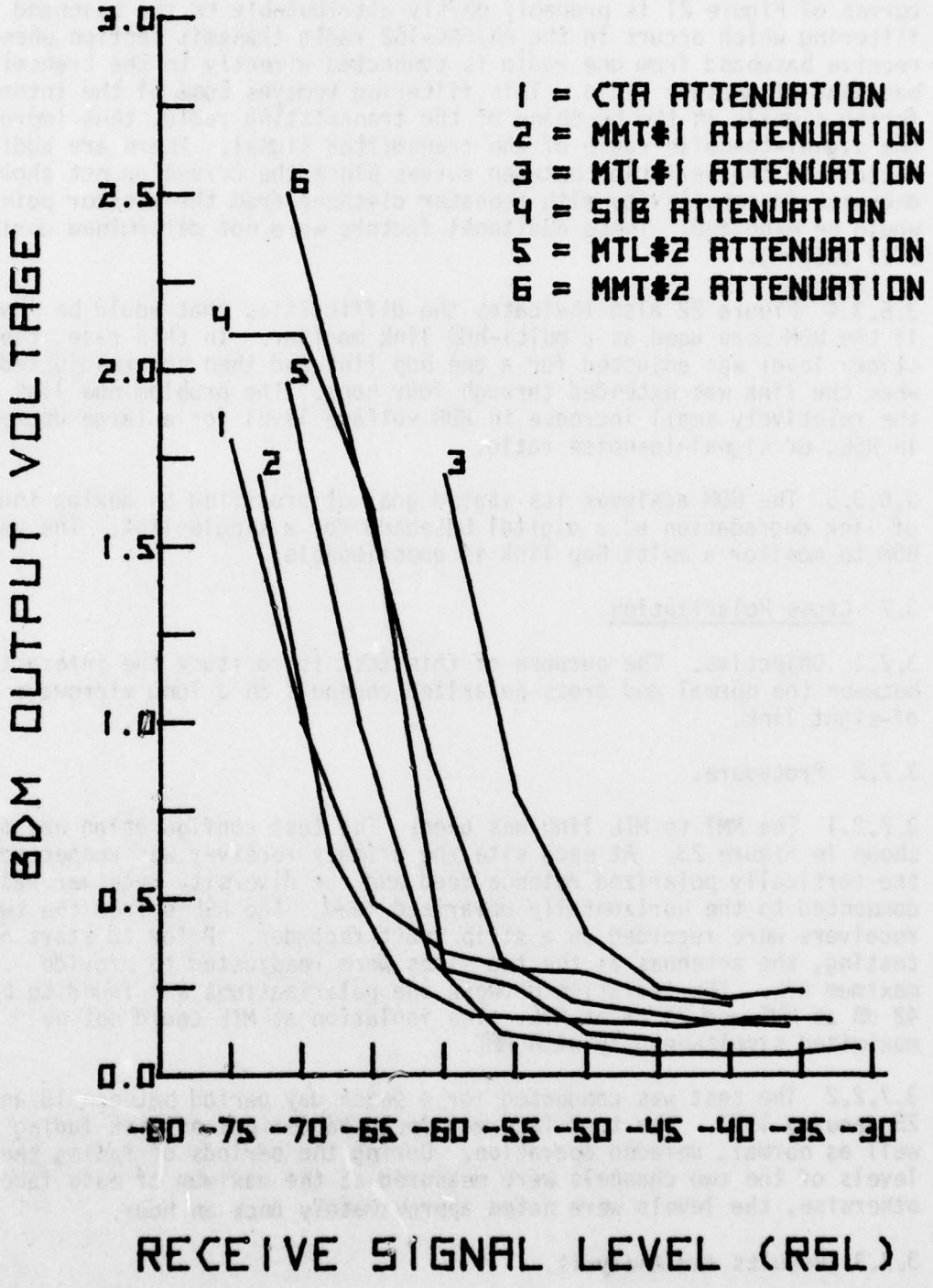

Figure 21. BDM Response for Six Hops

would require immediate corrective action. The wide variation in the curves of Figure 21 is probably partly attributable to the baseband filtering which occurs in the AN/FRC-162 radio transmit section when the receive baseband from one radio is connected directly to the transmit baseband of another radio. This filtering removes some of the interfering signals in the baseband of the transmitting radio, thus improving the signal-to-noise ratio of the transmitted signal. There are additional factors in the variation between curves since the curves do not show a decrease in sensitivity with repeater distance from the monitor point as would be expected. These additonal factors were not determined during DTEP testing.

3.6.3.4 Figure 22 also indicates the difficulties that would be involved if the BDM were used as a multi-hop link monitor. In this case, the BDM slicer level was adjusted for a one hop link and then not readjusted when the link was extended through four hops. The problem now lies in the relatively small increase in BDM voltage level for a large decrease in RSL, or signal-to-noise ratio.

3.6.3.5 The BDM achieves its stated goal of providing an analog indication of link degradation of a digital baseband for a single link. The use of BDM to monitor a multi-hop link is questionable.

3.7 Cross Polarization.

3.7.1 Objective. The purpose of this test is to study the interaction between the normal and cross-polarized channels on a long microwave line-of-sight link.

3.7.2 Procedure.

3.7.2.1 The MMT to MTL link was used. The test configuration was as shown in Figure 23. At each site the primary receiver was connected to the vertically polarized antenna feed and the diversity receiver was connected to the horizontally polarized feed. The RSL's from the two receivers were recorded on a strip chart recorder. Prior to start of testing, the antennas at the two sites were readjusted to provide maximum RSL. The isolation between the polarizations was found to be 42 dB at MMT and 25 dB at MTL. The isolation at MTL could not be maximized simultaneously with MMT.

3.7.2.2 The test was conducted for a seven day period between 18 and 25 January 1977. The test interval included periods of link fading as well as normal, unfaded operation. During the periods of fading the levels of the two channels were measured at the maximum of each fade; otherwise, the levels were noted approximately once an hour.

3.7.3 Results and Analysis.

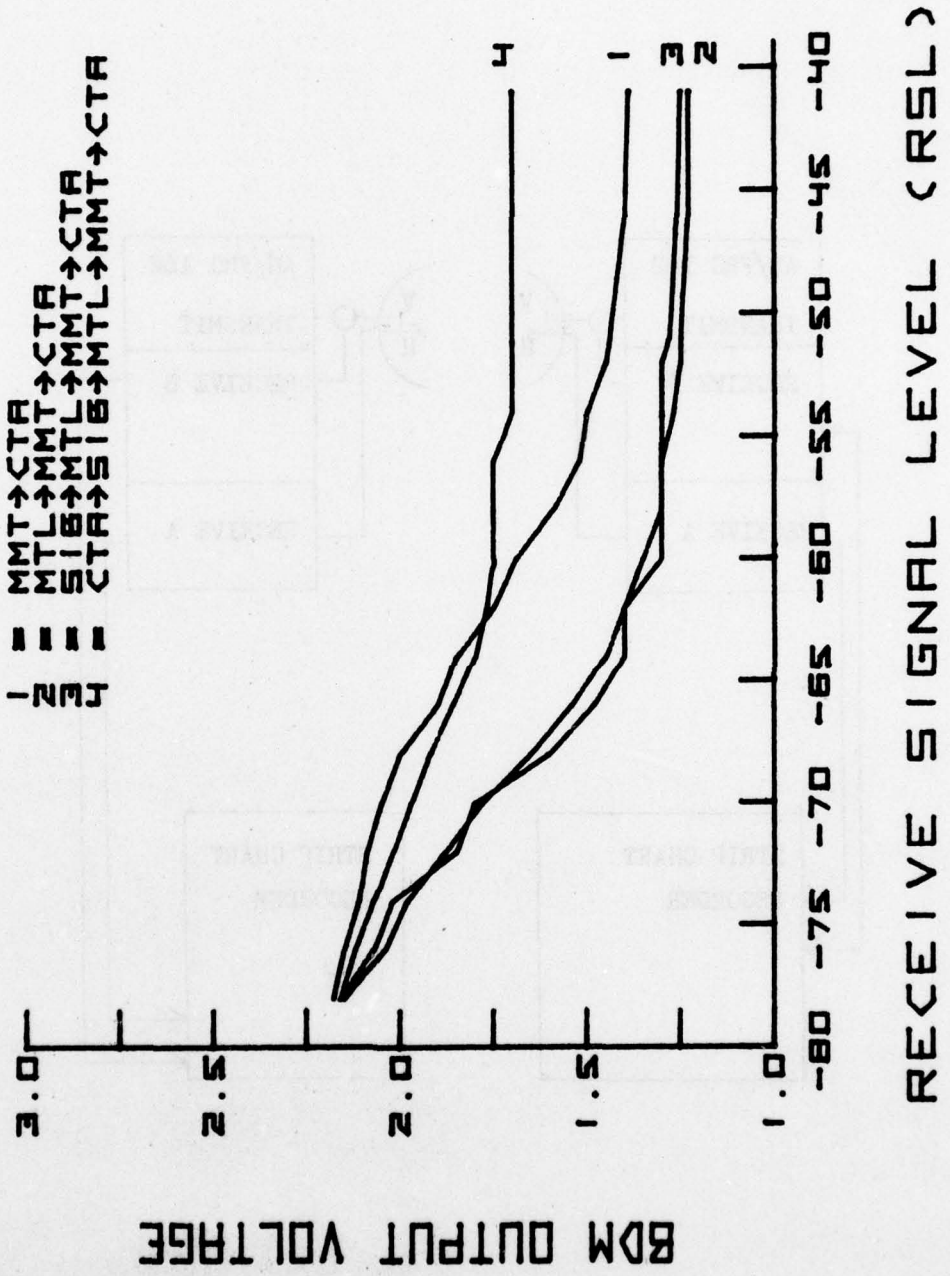

Figure 22. Multi-Hop BDM Response

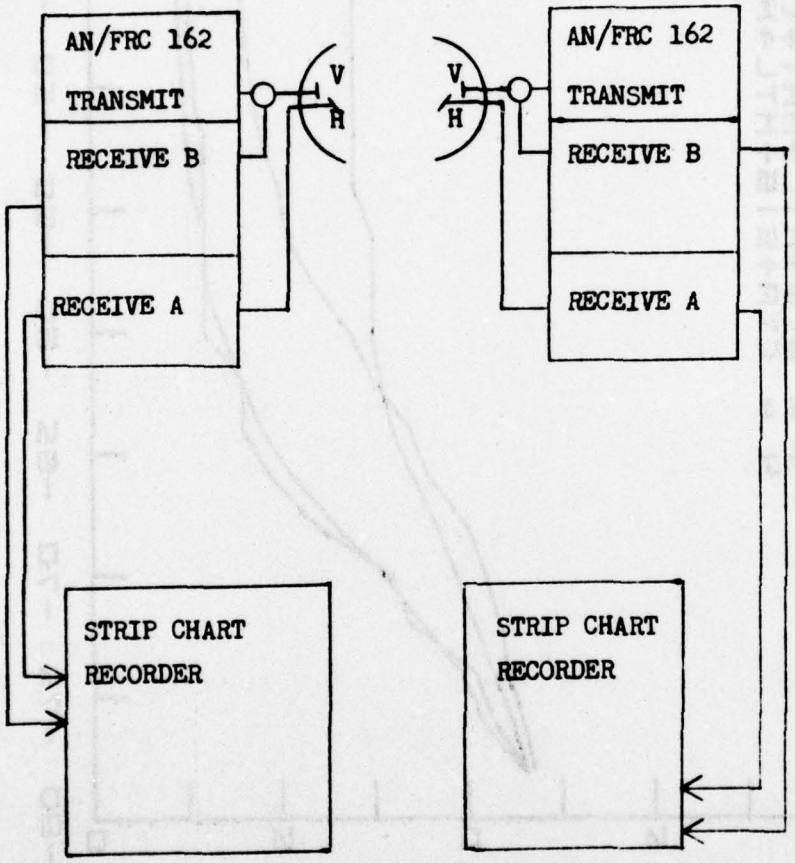

Figure 23. Test Configuration For Cross Polarization Test

3.7.3.1 Figures 24 and 25 show the distribution of cross-polarization isolation for MMT and MTL during periods of unfaded link operation. The spread of data is much larger for MMT than for MTL. The mean of the distribution for MTL is 25.7 dB with a standard deviation of 1.2 dB while the mean for MMT is 36.1 dB with a standard deviation of 3.7 dB.

3.7.3.2 Figure 26 shows the distribution of samples during periods of link fading for MTL. The behavior at MTL is little changed from the unfaded case; the mean decreased 1 dB to 24.7 dB while the standard deviation increased by 1.4 dB to 2.6 dB. Thus the level of isolation is not dependent on fade depth for MTL.

3.7.3.3 The distribution of samples does show a correlation with fade depth at MMT, as indicated in Figure 27. The line on the figure is based on a least-squares analysis using all of the data points in the figure. The correlation coefficient for this line is -0.559 which, for the degrees of freedom for the case, indicates an extremely high probability of correlation between fade depth and cross-polarized isolation levels. The standard error of estimate of the line is 6.7 dB.

3.7.3.4 There were five occurrences of abnormal fade behavior at MMT and three at MTL during this period. At these times the level of the cross-polarized channel was very close to or higher than the level of the other channel. Each case had two characteristics in common: first, the actual value of the RSL was less than -60 dBm for both channels; and second, the fade rate for both channels was close to the maximum rate at which the RSL could be tracked.

3.8 Wideband Noise Quieting.

3.8.1 Objective. The purpose of this test is to determine the noise behavior of the AN/FRC-162 at the input to the T1-4000 multiplexer.

3.8.2 Procedure. The CTA to MMT link was utilized with the link RSL varied between -30 dBm and -80 dBm and measurements made of the corresponding noise level at the multiplexer input. The passband characteristics of the baseband filter and the high pass output filter of the multiplexer were also measured.

3.8.3 Results and Analysis.

3.8.3.1 Figures 29 through 33 show the noise quieting curves at five different frequencies in the multiplexer passband. Figures 29 through 33 show that for frequencies between 1248 KHz and 5340 KHz, the FM thermal noise quieting region extends from approximately -30 dBm to -65 dBm. This type of behavior is normal for a radio without pre-emphasis. Figure 29 for a 70 KHz noise slot, shows that baseband spillover

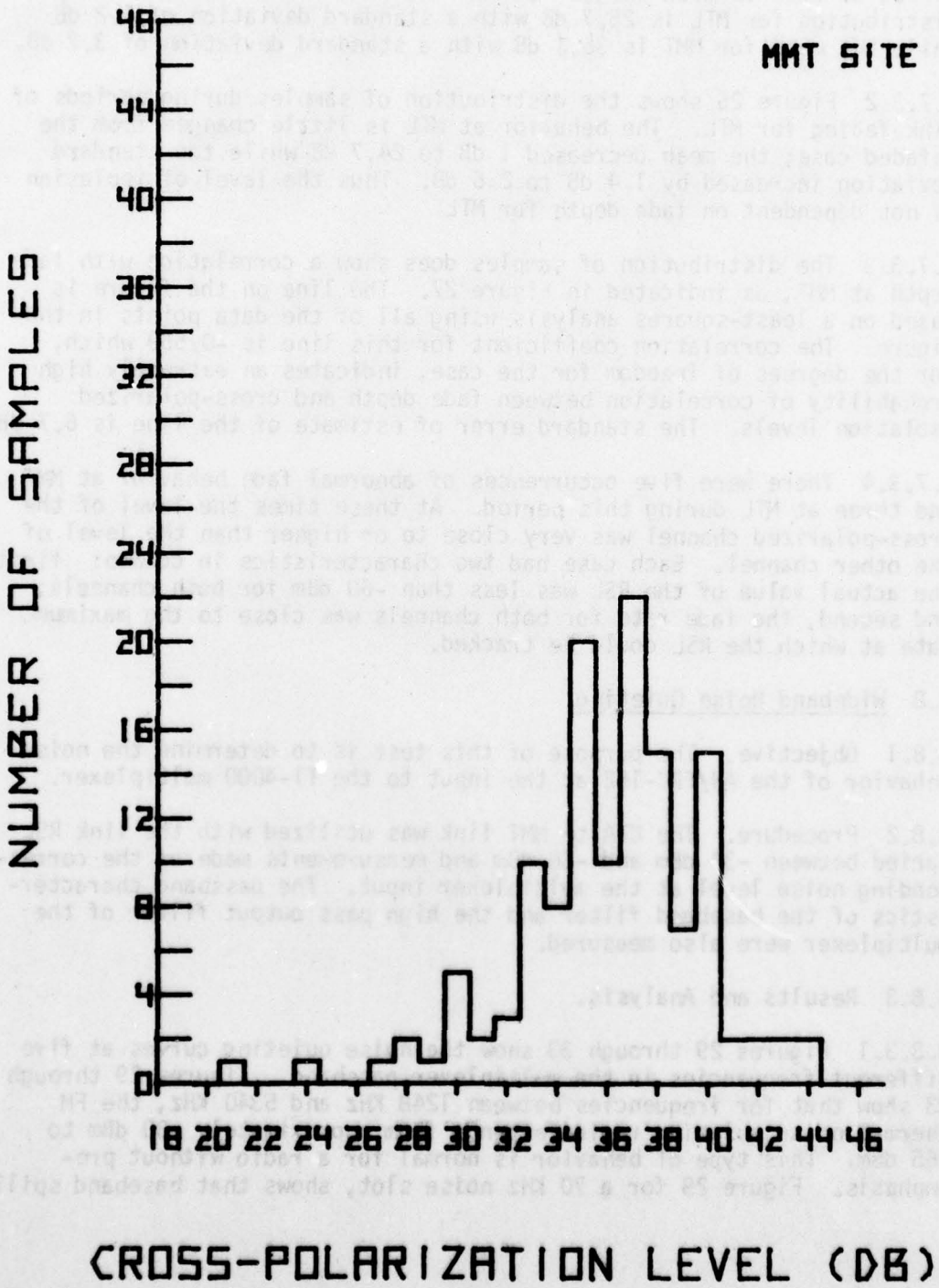

Figure 24. Cross Polarization Distribution for MMT

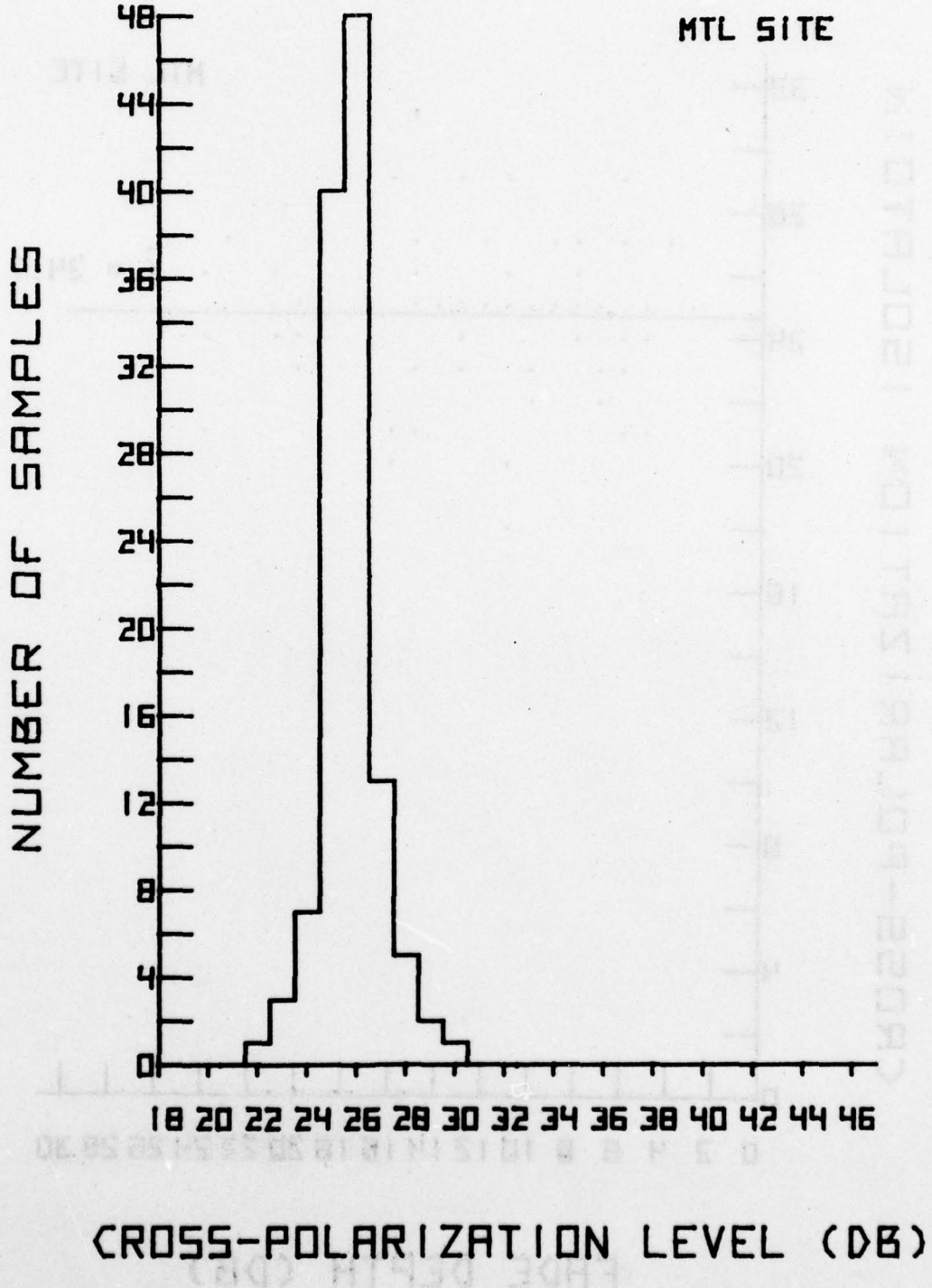

Figure 25. Cross Polarization Distribution for MTL

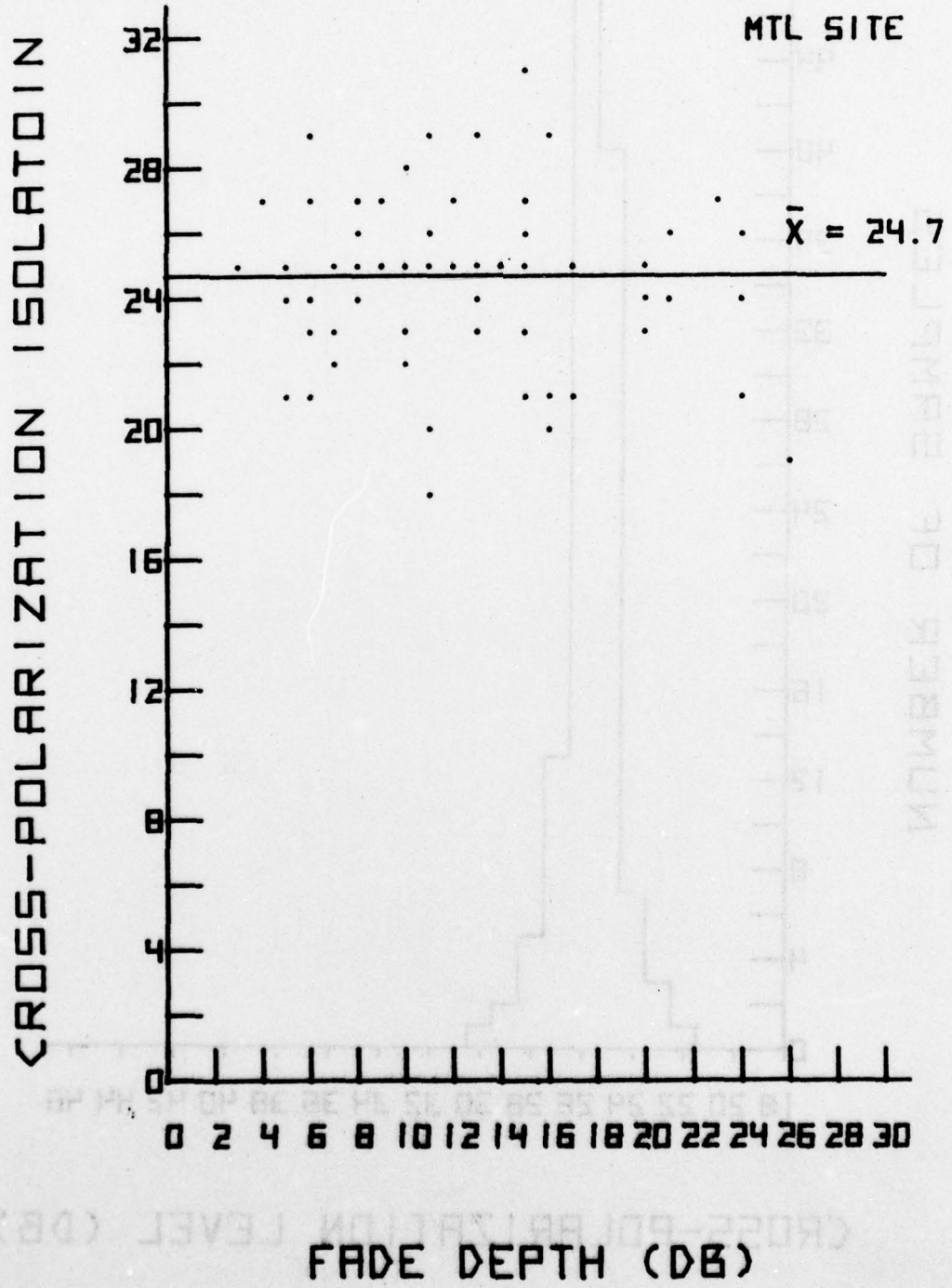

Figure 26. Faded Link Cross Polarization Isolation MTL

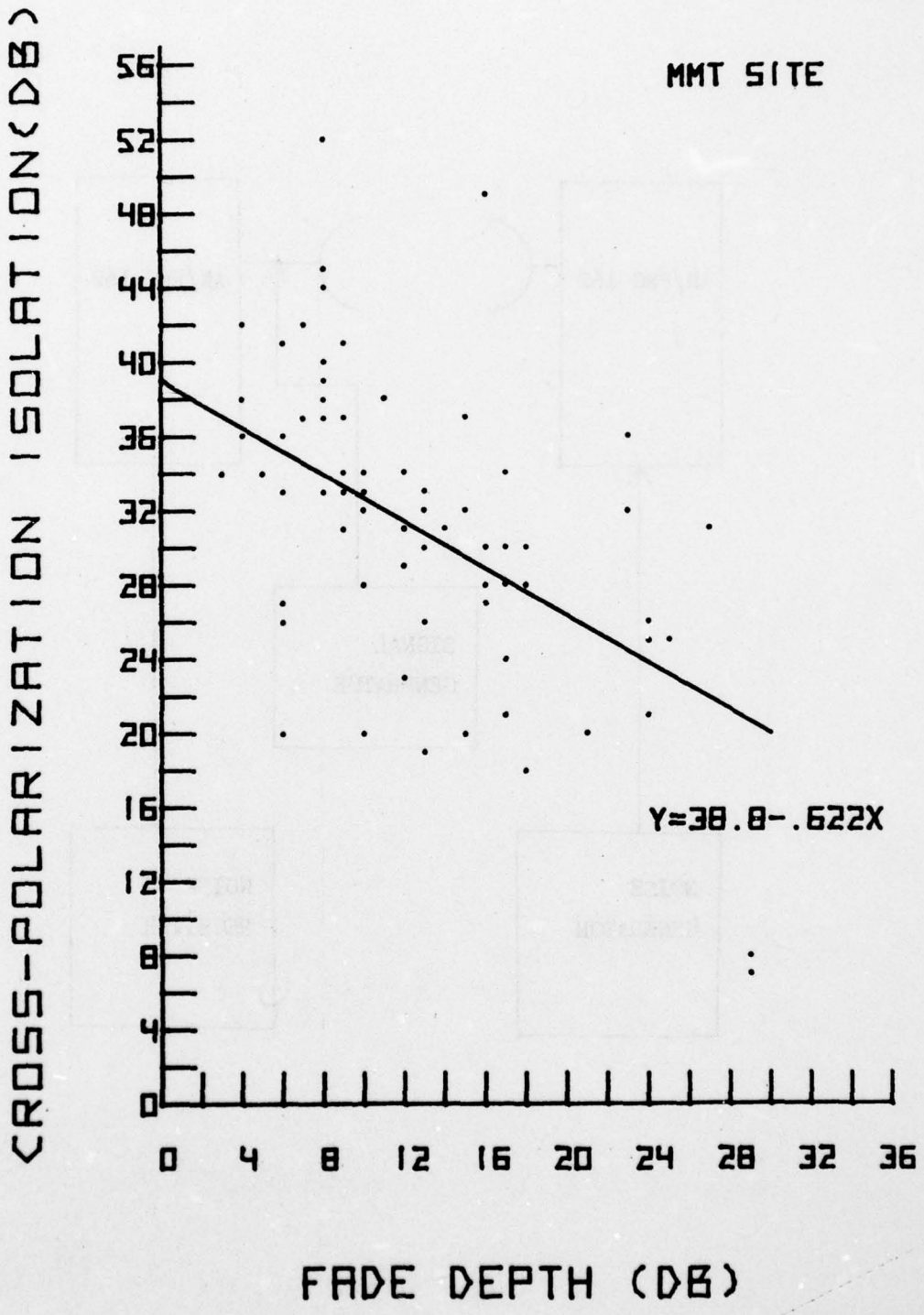

Figure 27. Faded Link Cross Polarization Isolation MMT

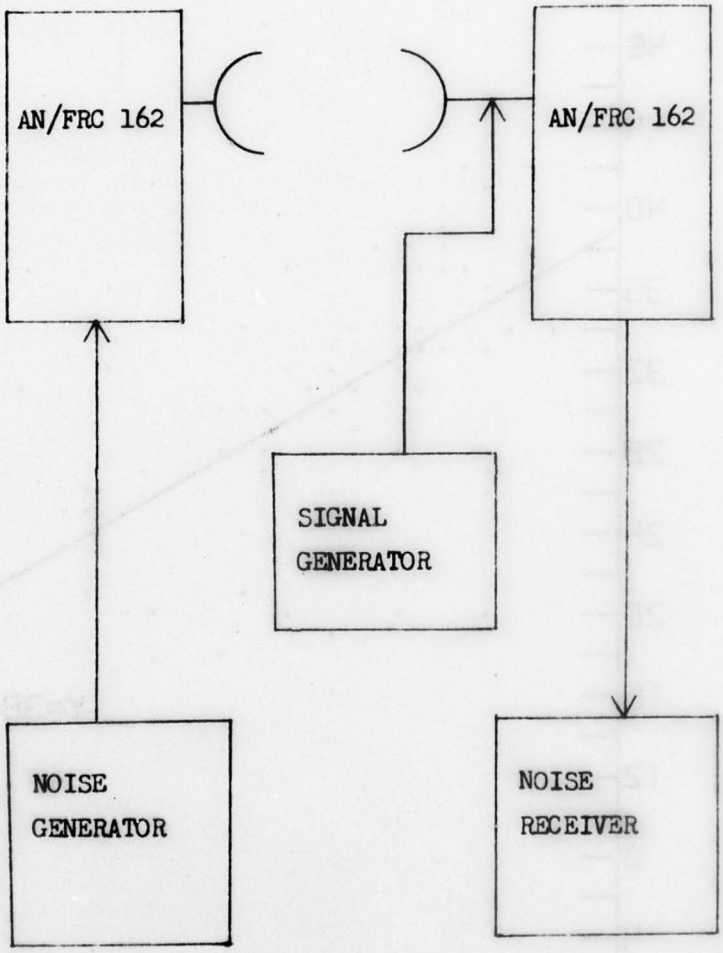

Figure 28. Test Configuration for Wideband Noise Quieting

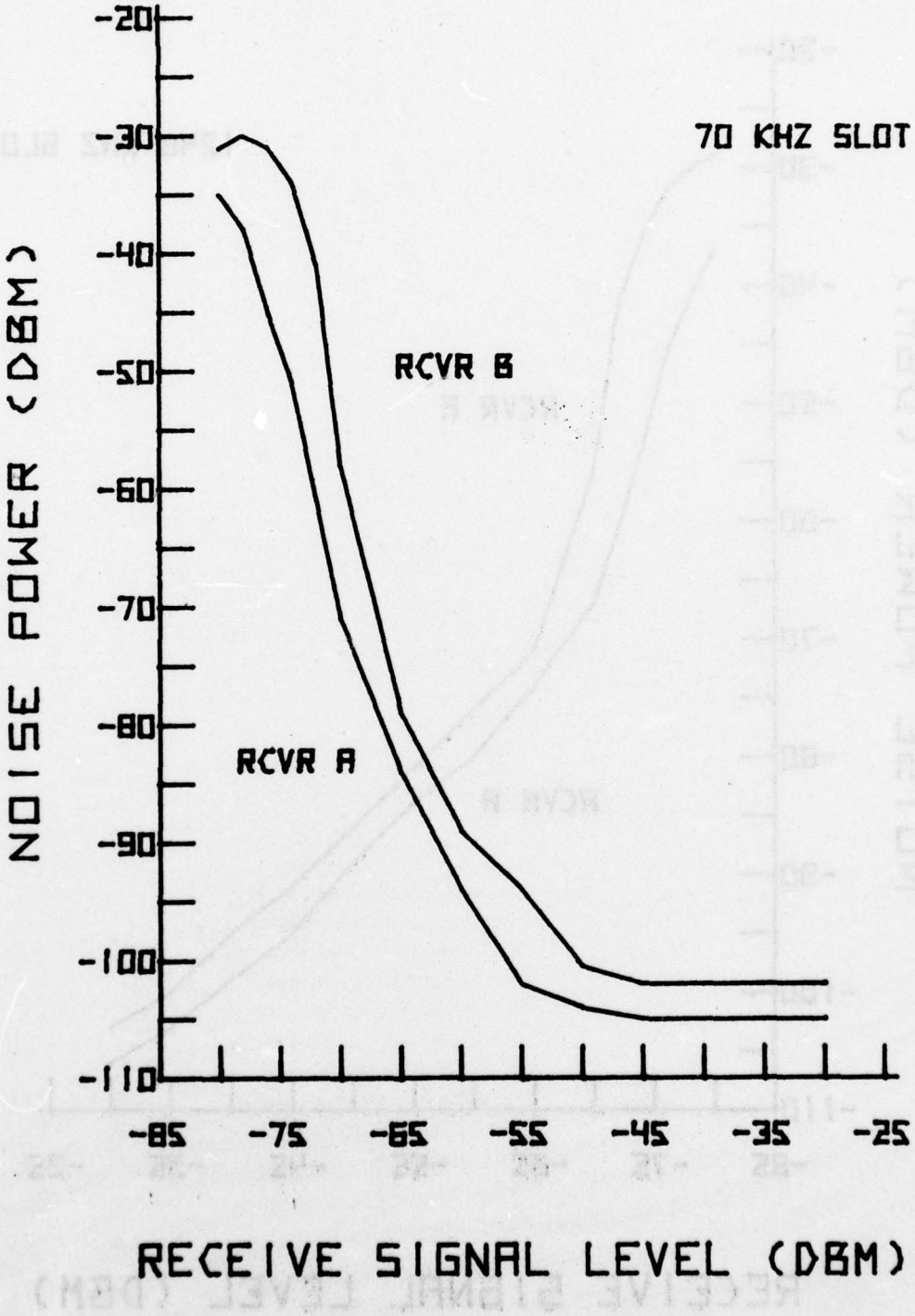

Figure 29. Noise Quieting Curve for 70 KHz Slot

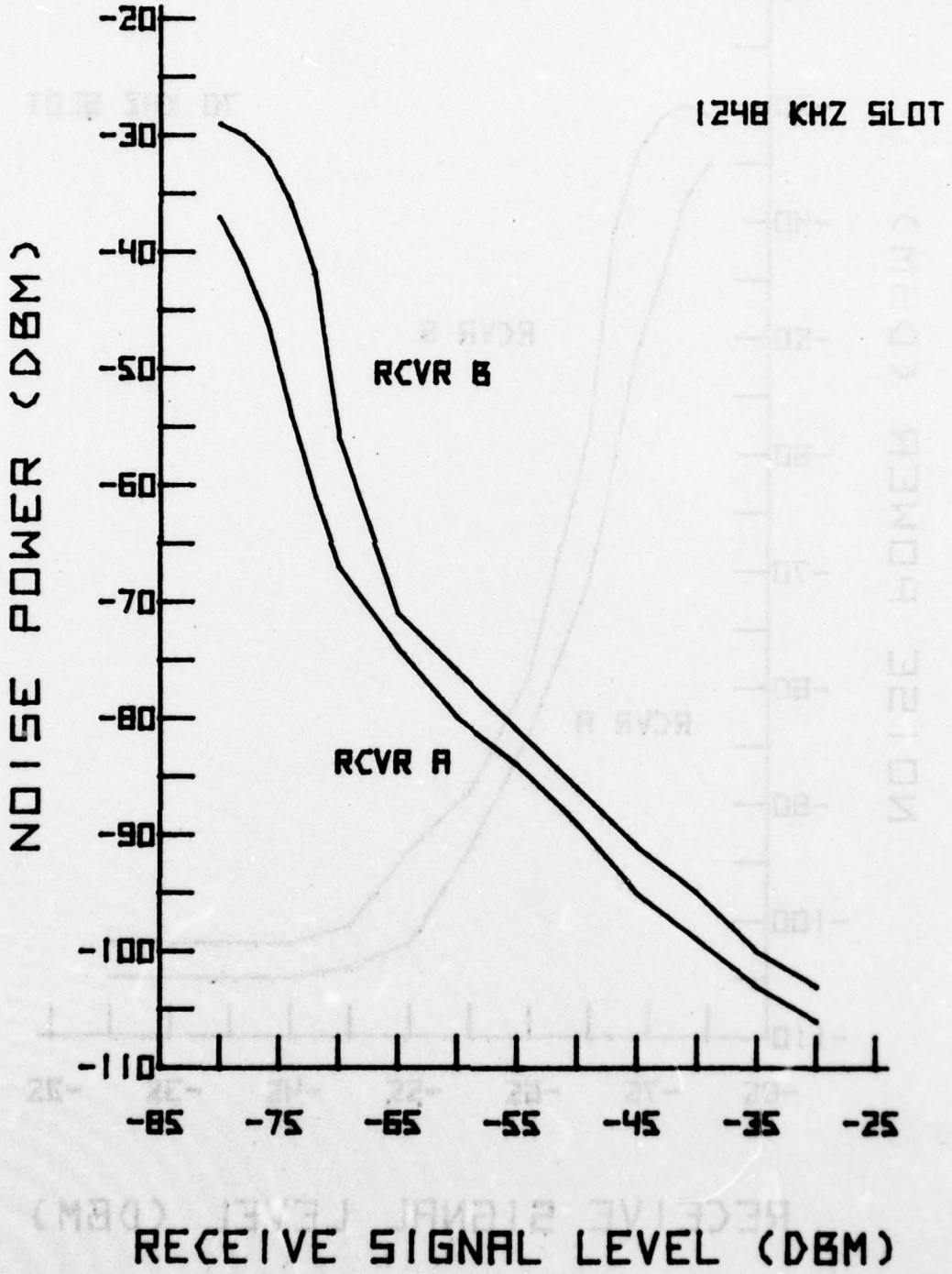

Figure 30. Noise Quieting Curve for 1248 KHz Slot

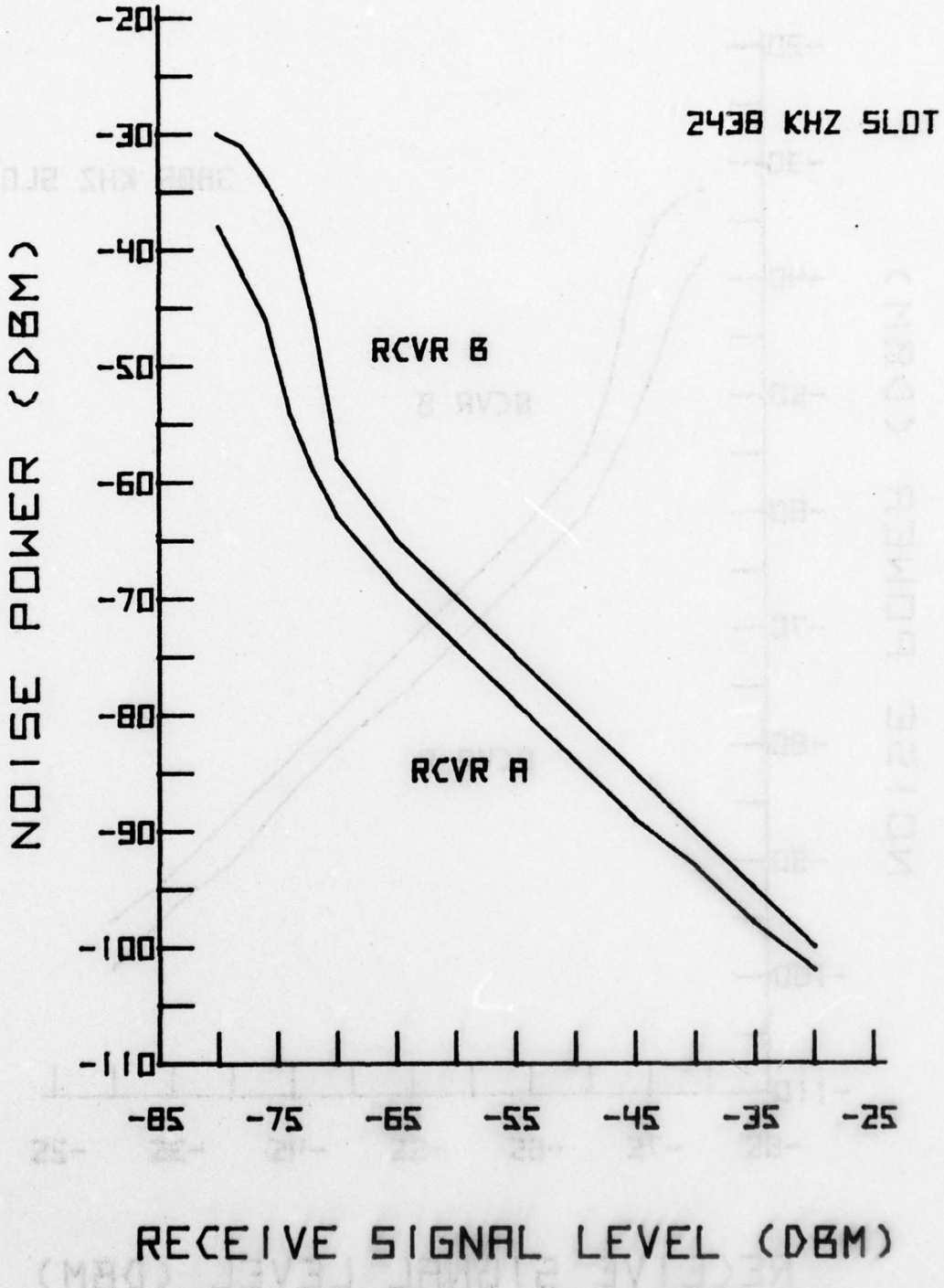

Figure 31. Noise Quieting Curve for 2438 KHz Slot

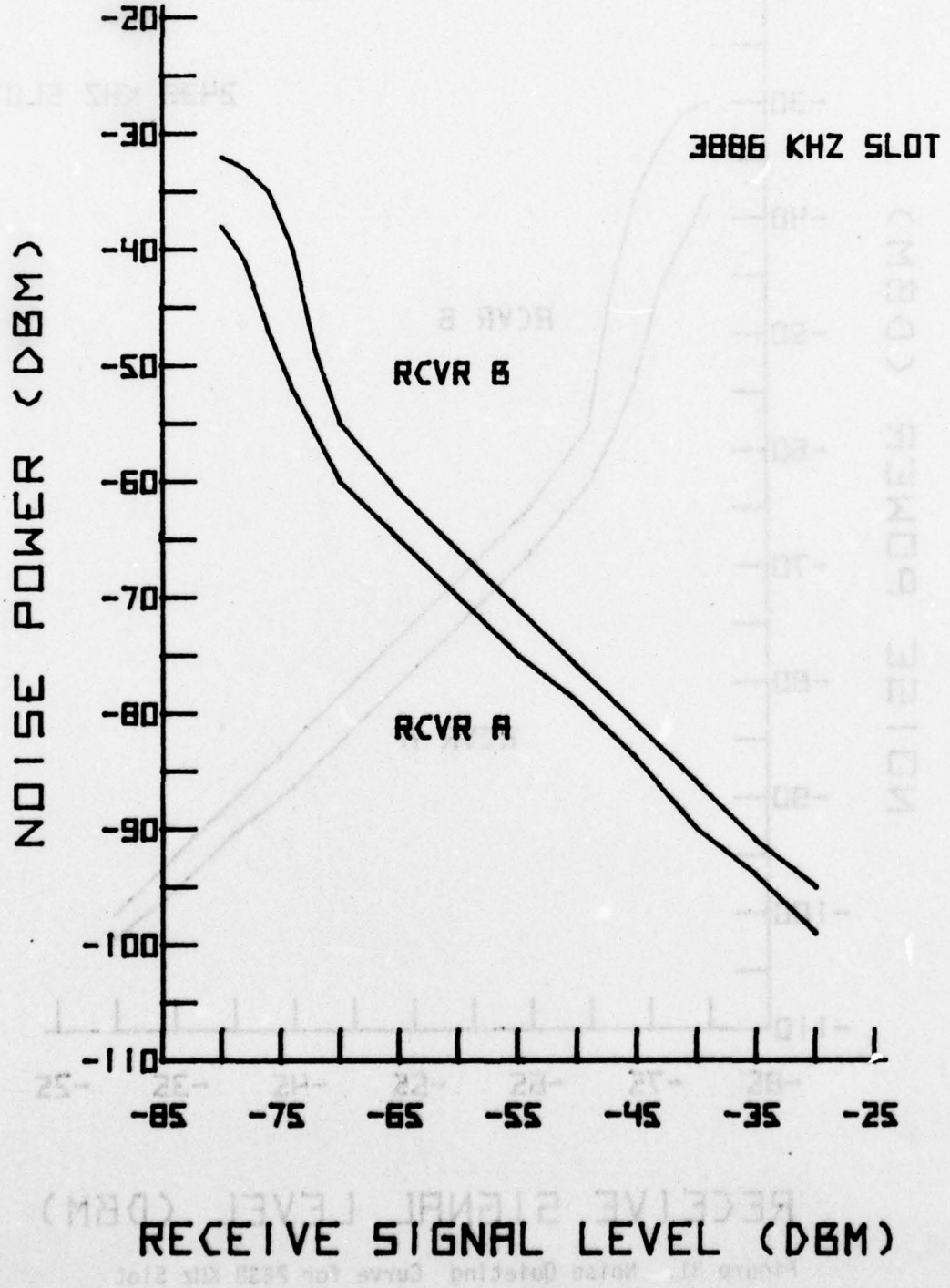

Figure 32. Noise Quieting Curve for 3886 KHz Slot

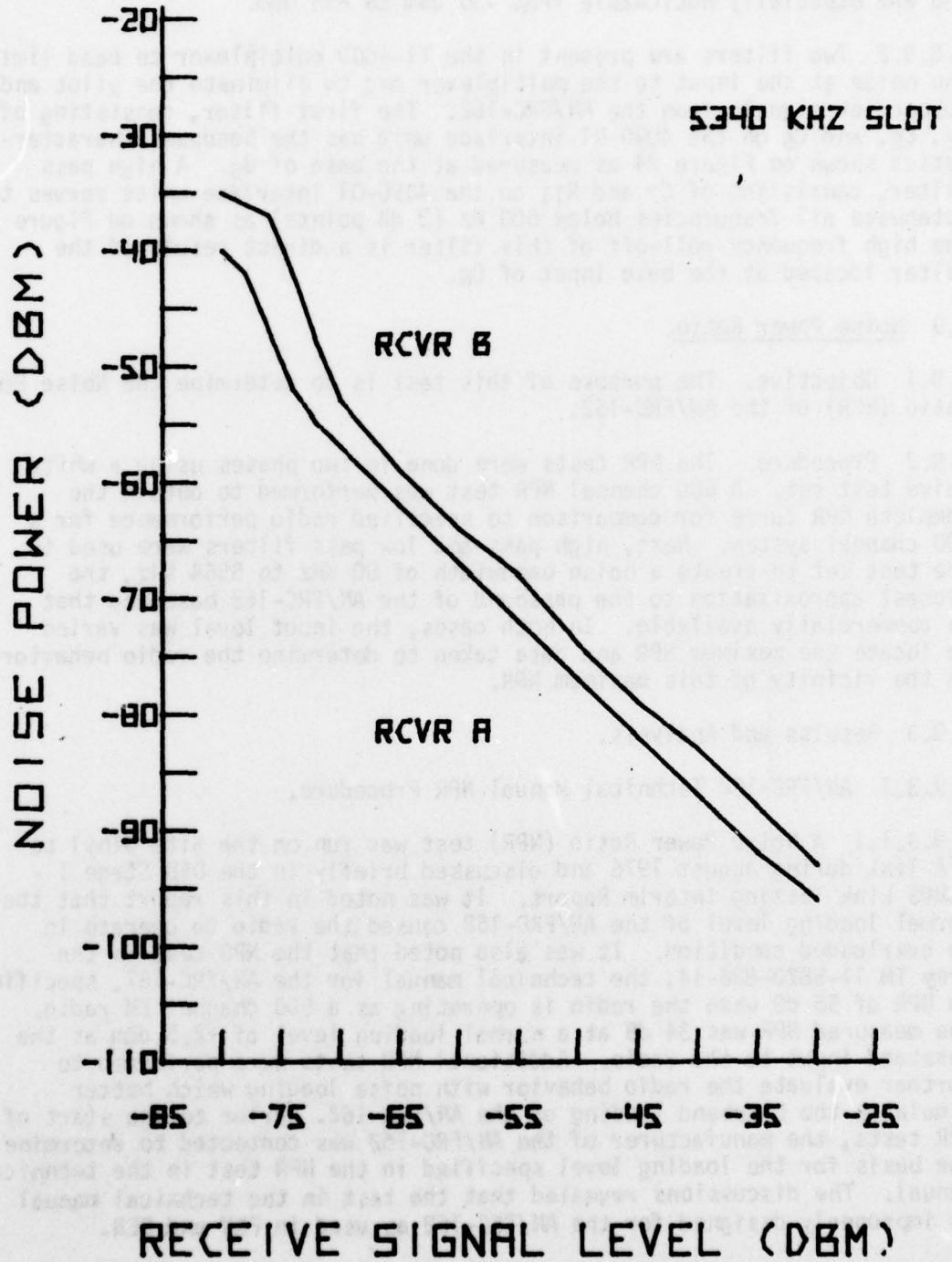

Figure 33. Noise Quieting Curve for 5340 KHz Slot

and intermodulation products predominate throughout the entire RSL range and are especially noticeable from -30 dBm to -55 dBm.

3.8.3.2 Two filters are present in the T1-4000 multiplexer to band limit the noise at the input to the multiplexer and to eliminate the pilot and subcarrier signals from the AN/FRC-162. The first filter, consisting of L_2, C_5, and C_6 on the 4090-01 interface unit has the bandpass characteristics shown on Figure 34 as measured at the base of Q_6. A high pass filter, consisting of C_7 and R_{11} on the 4090-01 interface units serves to attenuate all frequencies below 600 Hz (3 dB points) as shown on Figure 35. The high frequency roll-off of this filter is a direct result of the filter located at the base input of Q_6.

3.9 Noise Power Ratio.

3.9.1 Objective. The purpose of this test is to determine the Noise Power Ratio (NPR) of the AN/FRC-162.

3.9.2 Procedure. The NPR tests were done in two phases using a white noise test set. A 600 channel NPR test was performed to obtain the complete NPR curve for comparison to specified radio performance for a 600 channel system. Next, high pass and low pass filters were used in the test set to create a noise bandwidth of 60 KHz to 5564 KHz, the closest approximation to the passband of the AN/FRC-162 baseband that is commercially available. In both cases, the input level was varied to locate the maximum NPR and data taken to determine the radio behavior in the vicinity of this maximum NPR.

3.9.3 Results and Analysis.

3.9.3.1 AN/FRC-162 Technical Manual NPR Procedure.

3.9.3.1.1 A Noise Power Ratio (NPR) test was run on the Site Sibyl to CTA link during August 1976 and discussed briefly in the DEB Stage I - CONUS Link Testing Interim Report. It was noted in this report that the normal loading level of the AN/FRC-162 caused the radio to operate in an overloaded condition. It was also noted that the NPR test in the Army TM 11-5820-836-14, the technical manual for the AN/FRC-162, specifies an NPR of 55 dB when the radio is operating as a 600 channel FM radio. The measured NPR was 34 dB at a normal loading level of +2.5 dBm at the baseband input to the radio. Additional NPR tests were performed to further evaluate the radio behavior with noise loading which better simulates the baseband loading of the AN/FRC-162. Prior to the start of NPR tests, the manufacturer of the AN/FRC-162 was contacted to determine the basis for the loading level specified in the NPR test in the technical manual. The discussions revealed that the test in the technical manual is improperly designed for the AN/FRC-162 as used in FKV and DEB.

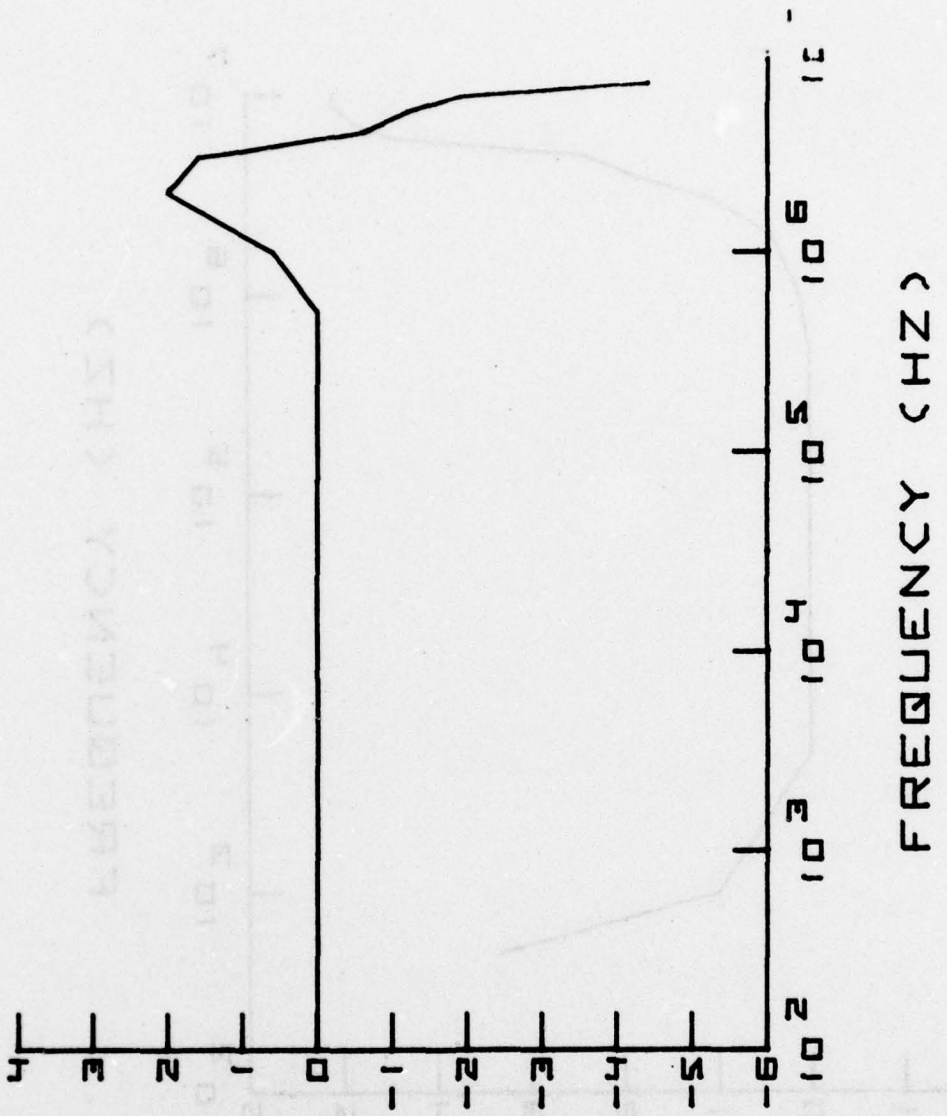

Figure 34. Multiplex Response at Q6

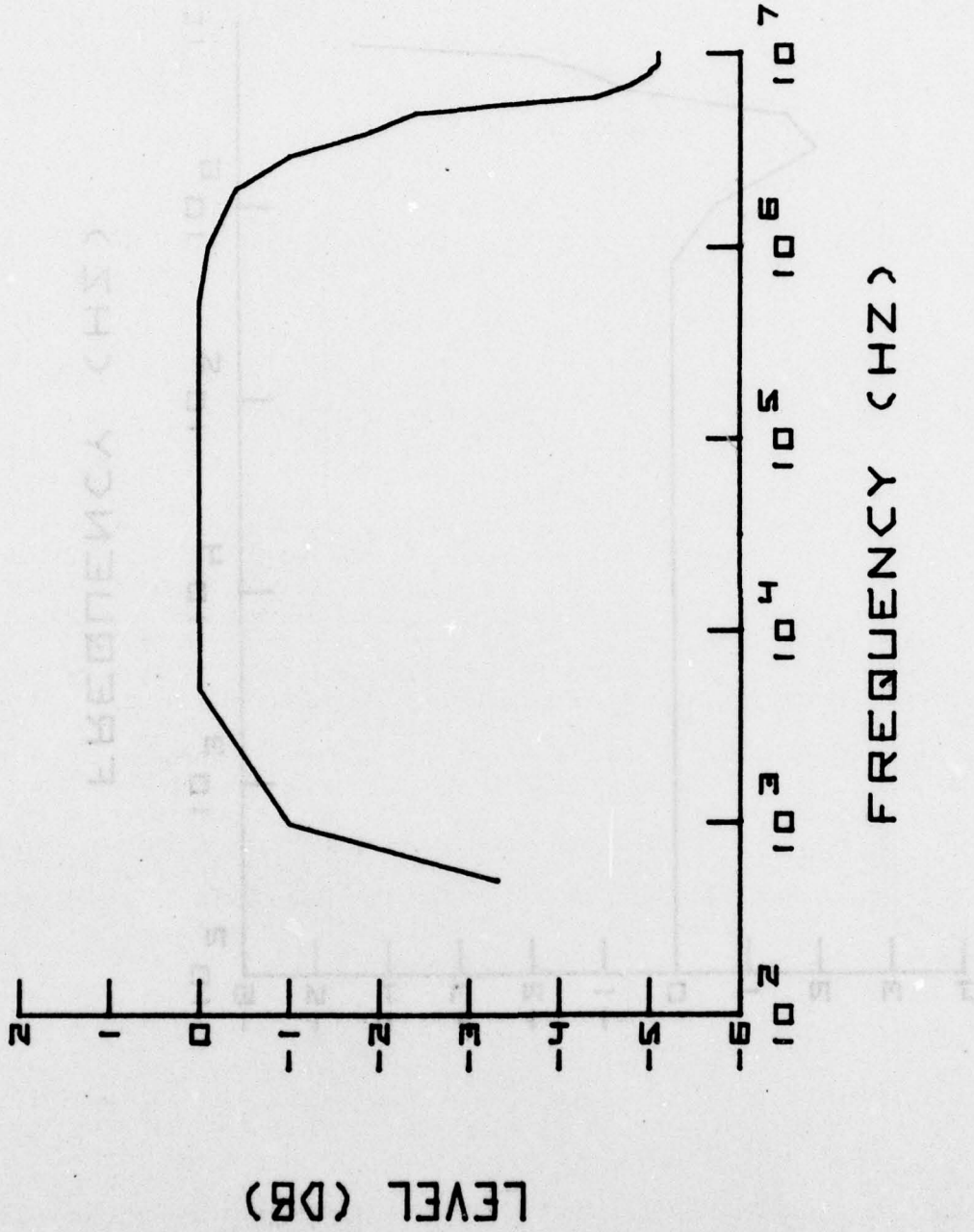

Figure 35. Multiplex Response at High Pass Filter

3.9.3.1.2 When performing an NPR test, the noise power to be inserted at the test level point (TLP) - in this case the baseband input to the radio receiver - is calculated from the DCA formula for "military" loading:

P = (-10 + 10 log N) dBm0

P = Noise loading level at the TLP

N = Number of channels

dBm0 = Power level in reference to the nominal loading level of the radio

DBm0 for the AN/FRC-162 is +2.5 dBm. For a 600-channel radio, using the above equation, P is equal to +17.8 dBm0 or a level at the TLP of +20.3 dBm. The Technical Manual for the AN/FRC-162 lists a level of -28.2 dBm at the TLP when performing the NPR test.

3.9.3.1.3 It was found that the NPR test for the AN/FRC-162 was identical to the NPR test described in the technical manual for the AN/FRC-155 radio set which is produced by the same manufacturer. The duplication is the result of the fact that components of the two radio sets which determine NPR performance are identical. The circuitry between the modulation amplifier input and transmitter RF output and between the RF input and the receiver IF amplifier output is the same for the two radios. The circuitry beyond these points is not identical. This is the key point in the difference in the NPR test procedures for the two radios.

3.9.3.1.4 The dBm0 for AN/FRC-155 is -45 dBm which, through amplification and attenuation, results in a level of -40 dBm at the input to the modulation amplifier. The AN/FRC-162 TLP of +2.5 dBm results in a level of -16 dBm at the input of the modulation amplifier. A loading level of +17.8 dBm0 at the TLP of the AN/FRC-155 would result in a baseband input level of -45 dBm +17.8 dB, or -27.2 dBm. The manufacturer's NPR test uses a voltmeter with a measurement inaccuracy of 1 dB, so the actual baseband input level is -28.2 dBm, the level listed in the Technical Manual for both radios.

3.9.3.1.5 As noted above, the AN/FRC-155 and AN/FRC-162 differ in the net gain between the baseband input and the modulation amplifier input. To determine the correct loading level for the NPR test of the AN/FRC-162 requires that the -40 dBm modulation amplifier input level be reflected back to the baseband input. To reduce the normal -16 dBm input level of the modulation amplifier to -40 dBm requires a 24 dB reduction of the baseband input level to -21.5 dBm. Adding +17.8 dBm0 to this level to obtain the proper level at the TLP for a 600 channel NPR test results in a loading level of -3.7 dBm at the baseband input to the AN/FRC-162.

3.9.3.2 Figures 36 and 37 show a typical NPR curve for the AN/FRC-162 radios on the Mule Mountain to CTA link at CTA for a 600 channel configuration. The expanded scale drawing of Figure 39 was used for analysis purposes as described below. It will be noted from the figures that the maximum NPR was greater than 55 dB in the 70 KHz slot at a level of -13.7 dBm0 (-11.2 dBm) at the TLP. At the normal loading level of +2.5 dBm, the NPR varied between 29 dB in the 70 KHz slot and 30 dB in the 2438 KHz slot.

3.9.3.3 Figure 38 shows a typical NPR curve for the AN/FRC-162 radios on the MMT to CTA link at MMT with a noise loading bandwidth of 60 KHz to 5564 KHz. The maximum NPR in the 70 KHz slot was 59 dB at a level of -7.7 dBm0 (-5.2 dBm) at the TLP. At the normal loading level of +2.5 dBm, the NPR varied between 40 dB in the 70 KHz slot and 35 dB in the 5340 KHz slot. The baseband shaping of the An/FRC-162 and the wide bandwidth (outside of normal test equipment limits) render any attempt to determine normal operating parameters of the radio such as signal-to-noise ratio, based upon the NPR, extremely difficult if not impossible.

3.9.3.4 The data obtained during the NPR test series was analyzed from two different standpoints to determine its validity. The NPR curve in the vicinity of the maximum was analyzed using techniques described in an article of the Lenkurt Demodulator.[1] The Basic Intrinsic Noise Ratio (BINR) data obtained while taking NPR data was compared with data points from the linear region of the comparable receiver FM quieting curve.

3.9.3.4.1 A line tangent to the portion of the NPR curve to the left of maximum point should have a 1:1 slope and should intercept a line drawn vertically from the level associated with the NPR maximum at an NPR which is within ±0.5 dB of the BINR reading taken at the NPR maximum. For a 600 channel noise test, the idle intercept point for the 70 KHz slot (see Figure 37) was at an equivalent NPR of 55.5 dB; the BINR at the two measurement points bracketing this maximum were 56 dB. For the wideband (60 KHz-5569 KHz) NPR test, the idle intercept point for the 70 KHz slot (see Figure 37) was at an equivalent NPR of 59.7 dB; the BINR at the two measurement points bracketing this maximum were 60 dB and 61 dB.

3.9.3.4.2 With a valid low-slot bucket curve, it should be possible to isolate the second order intermodulation line by first obtaining the idle and higher order intermodulation line and then subtracting this line from the measured curve to obtain the second order intermodulation line.[1] The results are shown on Figure 37. The same procedure was on the 70 KHz slot NPR curve from the wideband NPR test. The second order intermodulation line thus derived, excluding the effects of echo distortion, should

[1] "Bucket Curves", Lenkurt Demodulator, March 1976, p 2-19; April 1976, p 20-31

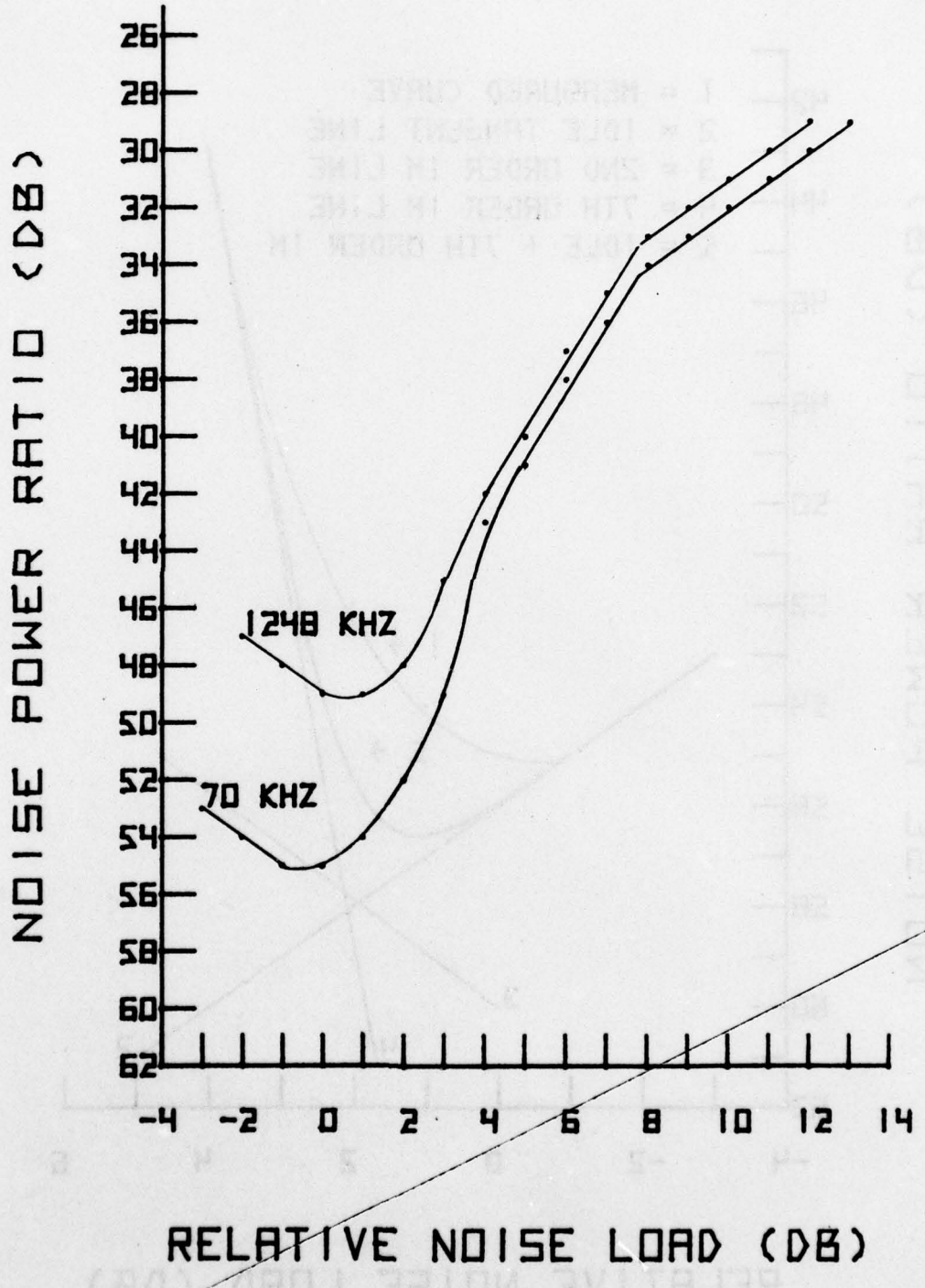

Figure 36. Noise Power Ratio vs Noise Load

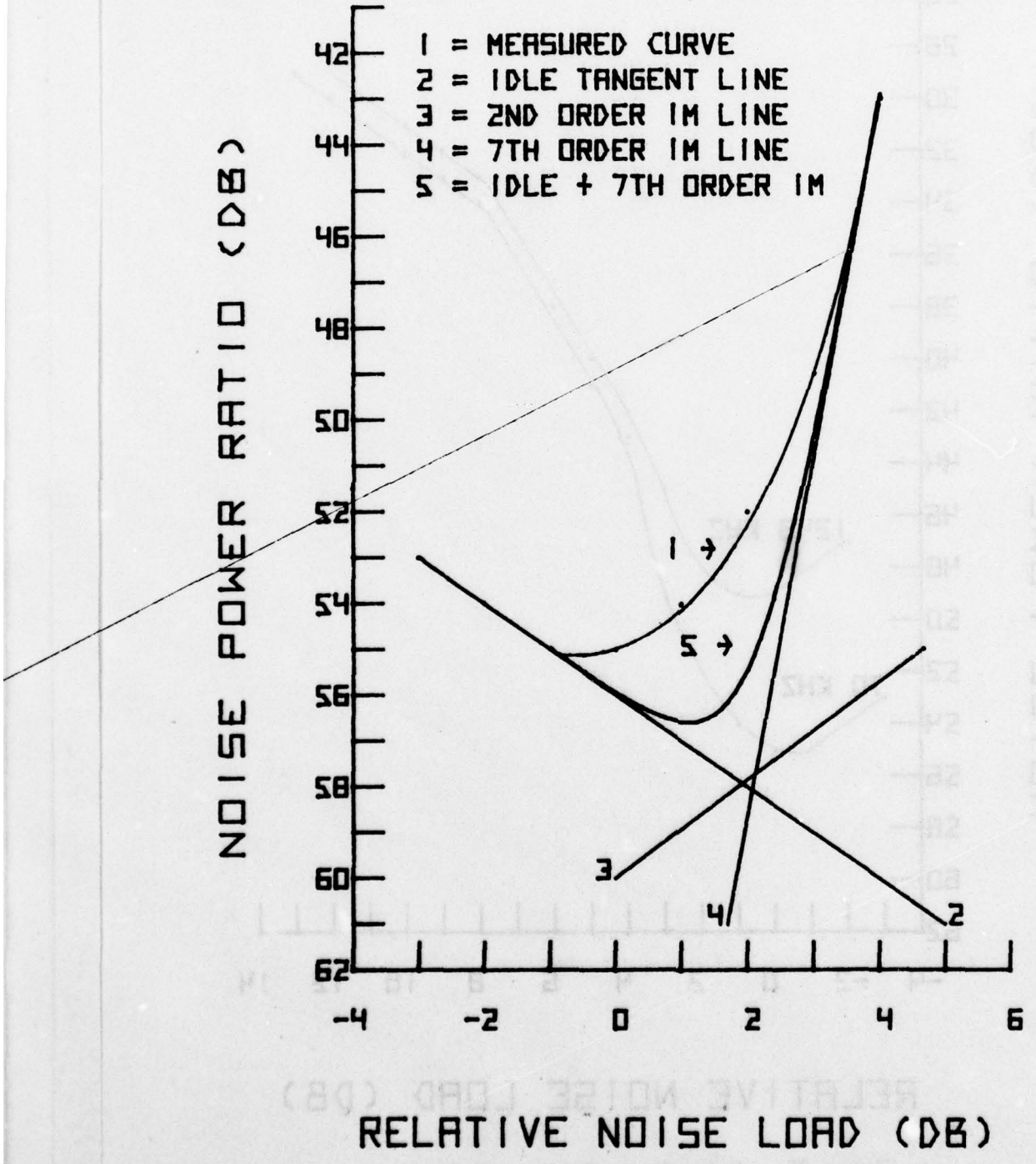

Figure 37. Expanded Noise Power Ratio vs Noise Load

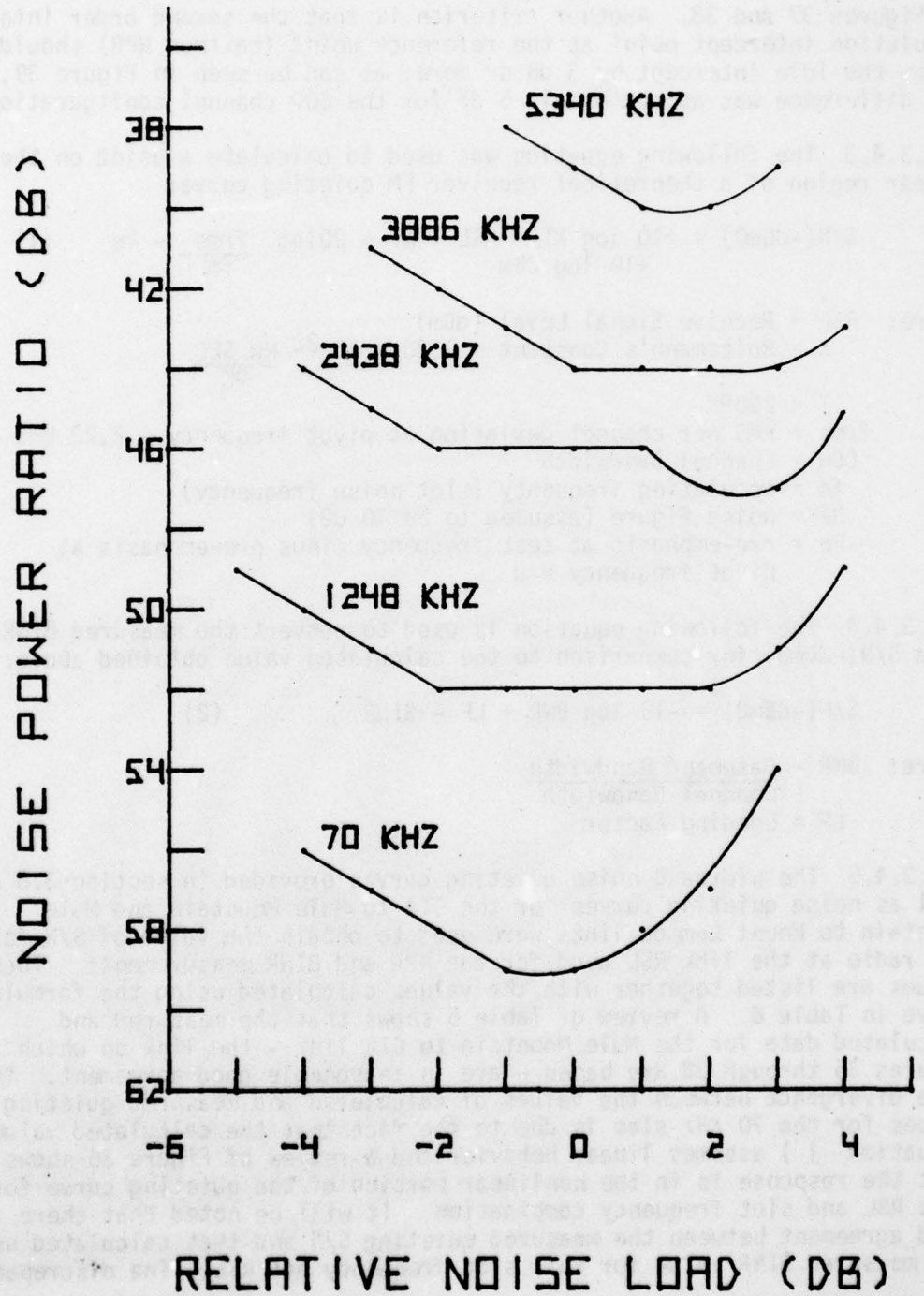

Figure 38. Noise Power Ratio vs Noise Load for 60 to 5340 KHz

have a slope of 1:1. This was found to be true of the low-slot curves on Figures 37 and 38. Another criterion is that the second order intermodulation intercept point at the reference point (maximum NPR) should be below the idle intercept by 3 dB or more; as can be seen in Figure 39, the difference was approximately 5 dB for the 600 channel configuration.

3.9.3.4.3 The following equation was used to calculate a point on the linear region of a theoretical receiver FM quieting curve:

$$S/N(-dBm0) = +10 \log KT + RSL + NF + 20\log \frac{frms}{fm} - Pe \quad (1)$$
$$+10 \log CBw$$

Where: RSL = Receive Signal Level (dBm)

K = Boltzmann's Constant = $1.38 \times 10^{-20} \frac{MW\ SEC}{^oK}$

T = 290^oK

frms = RMS per channel deviation at pivot frequency = 2.22 MHz

CBw = Channel Bandwidth

fm = modulating frequency (slot noise frequency)

NF = Noise Figure (assumed to be 10 dB)

Pe = pre-emphasis at test frequency minus pre-emphasis at pivot frequency = 0

3.9.3.4.4 The following equation is used to convert the measured BINR to a S/N(-dBm0) for comparison to the calculated value obtained above:

$$S/N(-dBm0) = -10 \log BWR + LF - BINR \quad (2)$$

Where: $BNR = \frac{\text{Baseband Bandwidth}}{\text{Channel Bandwidth}}$

LF = Loading Factor

3.9.3.4.5 The wideband noise quieting curves provided in section 3.8 as well as noise quieting curves for the CTA to Mule Mountain and Mule Mountain to Mount Lemmon links were used to obtain the value of S/N for the radio at the link RSL used for the NPR and BINR measurements. These values are listed together with the values calculated using the formulas above in Table 6. A review of Table 6 shows that the measured and calculated data for the Mule Mountain to CTA link - the link on which Figures 36 through 38 are based - are in reasonable good agreement. The wide divergence between the values of calculated and measured quieting values for the 70 KHz slot is due to the fact that the calculated value (equation 1) assumes linear behavior and a review of Figure 36 shows that the response is in the nonlinear portion of the quieting curve for this RSL and slot frequency combination. It will be noted that there is good agreement between the measured quieting S/N and that calculated using the measured BINR value for this slot frequency and RSL. The discrepancies

TABLE 6. Comparison of Measured and Calculated S/N

LINK	SLOT FREQ (KHz)	PSL (dBm)		Quieting S/N Measurement (-dBmØ)		Quieting S/N Calculation (-dBmØ)		BINR S/N Calculation (-dBmØ)		
		TxA	RxB	RxA	TxB	TxA	TxB	Loading Level (-dBmØ)	RxA	RxB
MMT-CTA		-42	-38	107.5	104.5	122	126	5.2	104.6	104
CTA-MMT	70	-39	-39	95.5	96.5	120.1	120.1	19.2	100.7	89.7
MMT-MTL		-35	-35	100.5	100.5	124.1	124.1	21.7	96.2	100.2
MMT-CTA		-42	-38	96.5	99.5	97	101	5.2	96.6	99.6
CTA-MMT	1248	-39	-39		100	95.1	95.1	19.2	94.7	94.7
MMT-MTL		-35	-35	98	97.5	99.1	99.1	21.7	102.2	103.2
MMT-CTA		-42	-38	94.0	94.5	94.5	91.2	5.2	91.6	90.6
CTA-MMT	2438	-39	-39	95.5	96	96	89.3	19.2	88.7	88.7
MMT-MTL		-35	-35	92.5	91.5	91.5	93.3	21.7	100.2	100.2
MMT-CTA		-42	-38	89.5	90.5	87.1	91.1	5.2		89.6
CTA-MMT	3886	-39	-39	92.5	92.0	85.2	85.2	19.2	84.7	74.7
MMT-MTL		-35	-35	89.5	89.5	89.2	89.2	21.7	97.2	98.2
MMT-CTA		-42	-38	87.5	87.5	84.4	88.4	5.2	82.6	85.6
CTA-MMT	5340	-39	-39	89.5	89.7	82.5	82.5	19.2	79.7	67.7
MMT-MTL		-35	-35	85.5	84.5	86.5	86.5	21.7	94.2	94.2

between measured and calculated values of S/N for the CTA to Mule Mountain and Mule Mountain to Mount Lemmon links were due to link disturbances during the test.

3.9.3.5 A review of Figure 36 shows that the NPR curve for the 600 channel configuration is broken into three separate divisons characterized by the slope of the curve to the right of the maximum NPR point. The first section, between loading levels of -13.7 dBm0 and -9.2 dBm0 has a slope of 8:1, indicating that seventh order intermodulation effects predominate in this region. The second section, between loading levels of -9.2 dBm0 and -5.2 dBm0 has a slope of 2:1, indicating that third order intermodulation effects predominate in this region. Between -5.2 dBm0 and 0 dBm0, the slope is 1:1, indicating that second order intermodulation effects predominate in this region, which is also the location of the normal loading point of the radio. The article previously referenced states that higher order slopes of 4:1 or greater are indicative of hard amplitude clipping or bandwidth truncation, probably the latter in this case.

3.9.3.6 An analysis of Figure 38 shows that the curve to the right of the maximum NPR also had a slope of 8:1, indicating that the behavior in this region for the wideband (60-5564 KHz) configuration was identical to that for the 600 channel configuration, i.e., seventh order intermodulation effects predominate.

3.9.3.7 As noted previously, the optimum calculated loading level for a 600 channel configuration of the AN/FRC-162 dBm is -3.7 dBm. The actual NPR maximum occurred at -11.2 dBm. If the wideband configuration is modeled as a 1260 channel system the optimum calculated loading level is -1.5 dBm, while the actual NPR maximum occurred at -5.2 dBm. These results indicate that the loading of the radio does not follow the normal loading equations, but is affected by the fact that the radio baseband is shaped rather than flat across the passband as assumed by the normal loading equations.

3.9.3.8 The NPR test procedure contained in the technical manual for the AN/FRC-162 is incorrect and should be eliminated. The specified value of 55 dB cannot be achieved at the baseband loading level of +2.5 dBm. The measurement of an NPR at the +2.5 dBm level is not as useful as a link delay or similar measurement made with a microwave link analyzer which better defines the performance of this radio.

APPENDIX A

Table 7 Terminal Equipment Specifications

SITE ABBREVIATION	LINK TO	TYPE EQUIPMENT	FREQUENCY (GHz) TRANS/RECEIVER	POWER (Watts)	TOWER HEIGHT (Ft) - ANTENNA HEIGHTS (Ft)	ANTENNA DIAMETER (Ft)	PATH LENGTH (Miles)	PREDICTED RECEIVE SIGNAL LEVEL (dBm)
CTA	SIB	AN/FRC-162	8.398/8.2975	1	60-39/19	8	32.1	-35
	MMT	AN/FRC-162	8.275/8.11	1	60-44/24	6	23.7	-41
SIB	CTA	AN/FRC-162	8.2975/8.398	1	60-39/19	8	32.1	-35
	MTL	AN/FRC-162	8.2045/8.3655	1	60-44/24	8	47.3	-40.7
MMT	CTA	AN/FRC-162	8.11/8.275	1	60-35/10	6	23.7	-41
	MTL	AN/FRC-165	8.2185/8.3795	5	60-46/20	12	82	-32
MTL	MMT	AN/FRC-165	8.3795/8.2185	5	80-66/36	12	82	-32
	SIB	AN/FRC-162	8.3655/8.2045	1	80-51/21	8	47.3	-40.7

APPENDIX B

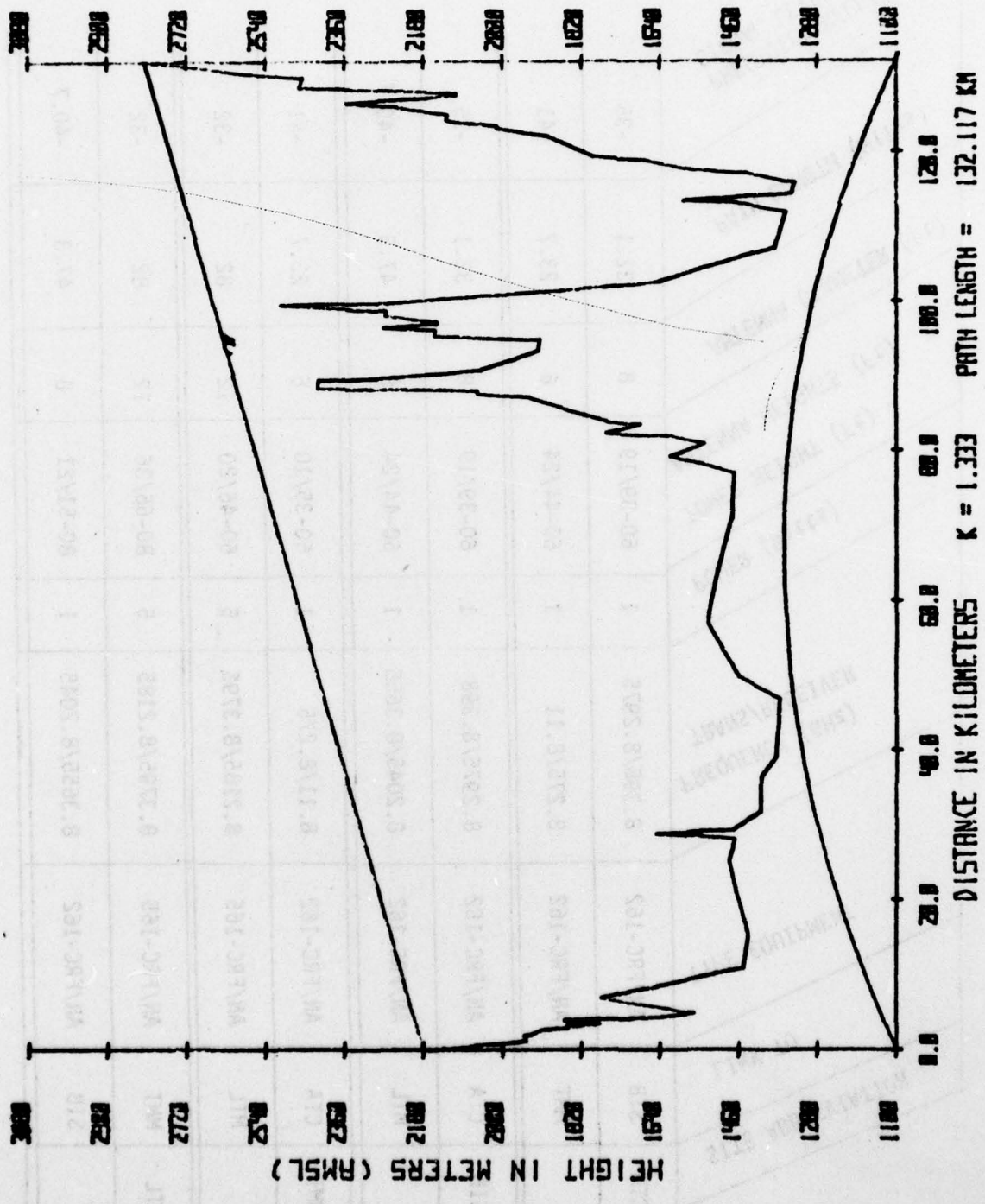

Figure 39. Mule Mountain-Mount Lemmon Path Profile (K=4/3)

APPENDIX B

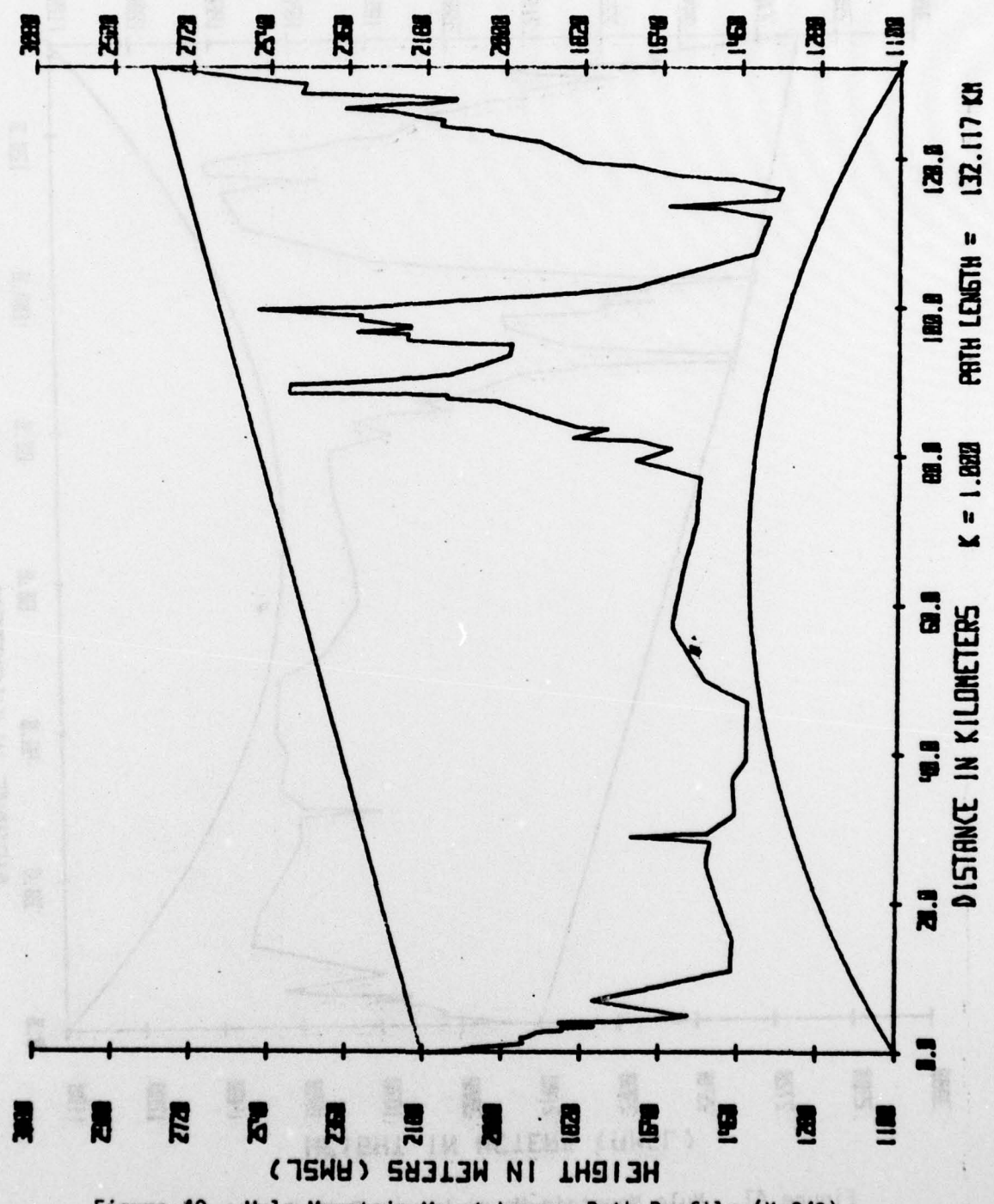

Figure 40. Mule Mountain-Mount Lemmon Path Profile (K=3/3)

APPENDIX B

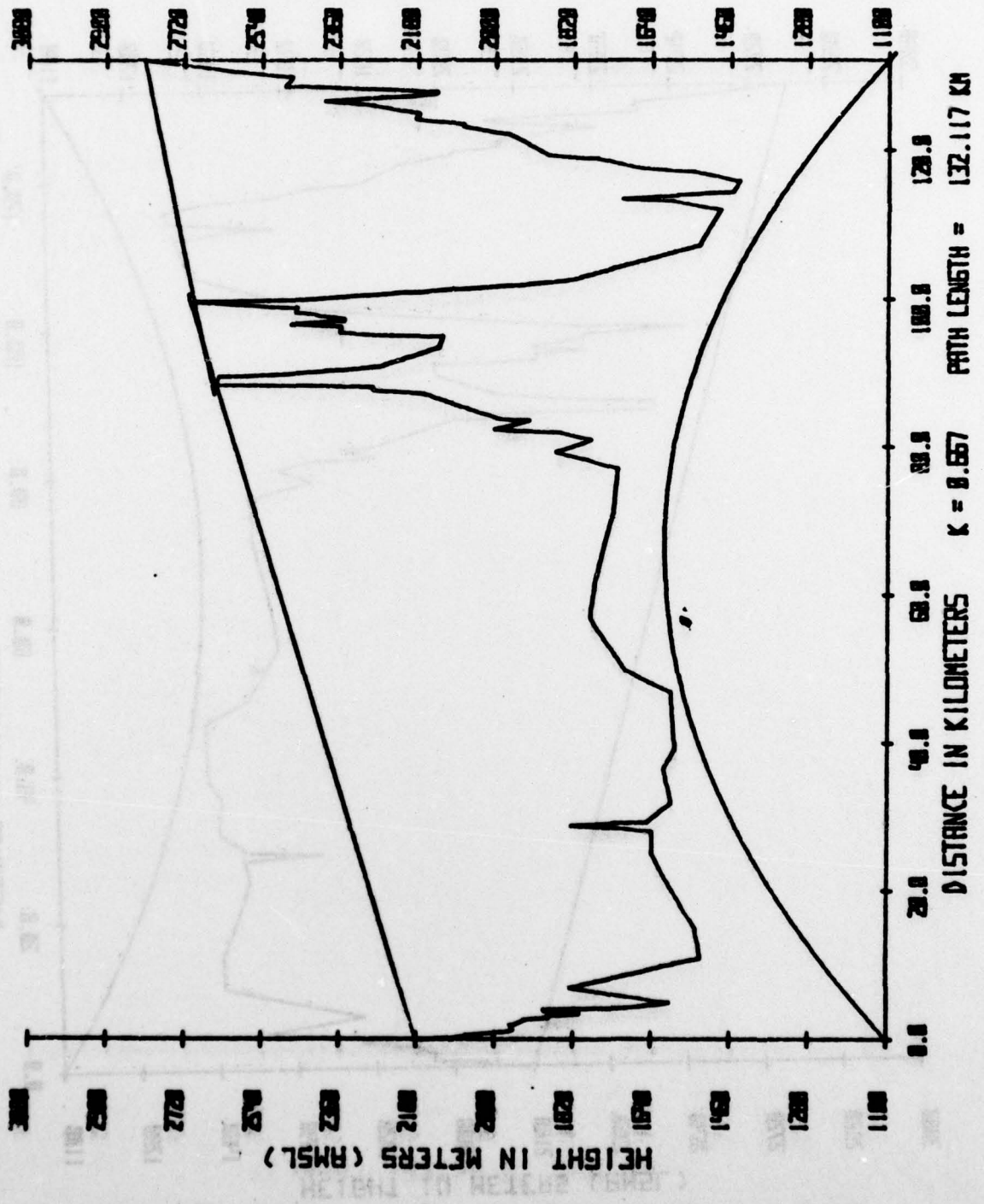

Figure 41. Mule Mountain-Mount Lemmon Path Profile (K-2/3)

APPENDIX C

AUTOMATIC DATA COLLECTION SYSTEM

At the start of the DEB CONUS link testing program, the test objectives required long term statistical information. This type of data was ideally suited to an automated data collection system approach. A system designed around a programmable calculator was proposed. Use of a programmable calculator reduces initial expenditures and provides system flexibility. The HP-9825A programmable calculator was procured for use as the system controller.

In addition to the calculator, the automatic data collection system consisted of the HP-IB, the HP-6940B Multiprogrammer, the HP-59500A Multiprogrammer interface, and bus controllable clock and timer, shown in Figure 42. The system interconnection is shown in Figure 43. The multiprogrammer was equipped with four voltage monitor cards, six pulse counter cards, and one event sense card. Details of the system interface with the Vicom T1-4000 multiplexer and the AN/FRC-162 radio are available upon request.

Data of interest centered around propagation performance: the depth, length and rate of path fading and the effect on bit error rate (BER); three level violation rate; mux reframe occurrences; and receiver switching actions. In order to record information on fast fades, samples had to be taken as quickly as possible. The original programming goal was one sample of AGC voltage every 50 msec. Since each site had two radios and each radio had two receivers, four AGC samples were required. These samples were then examined by the calculator to determine if activity was occurring. When activity occurred the sample was recorded along with a time indication. At a rate of four samples every 50 msec, all samples could not be recorded due to the lack of data storage space. In addition, counts of the number of errors, violations, and reframes for a set period of time were desired. A sample period for counts of one minute was selected to give a maximum measurable BER of 4×10^{-5}.

Program execution time prohibited the achievement of one sample of a receiver's AGC voltage every 50 msec. The slowest path through the calculator data collection program was found to be slightly less than 77 msec. Therefore, the system was set to take an AGC sample every 77 msec. This was done to insure time integrity for the samples.

The data collected which requires storage was placed in a string variable 2520 bytes in length. The position of the next storage byte was traced by a variable pointer to insure contiguous assignment. Whene

Figure 42. Photograph of Calculator System

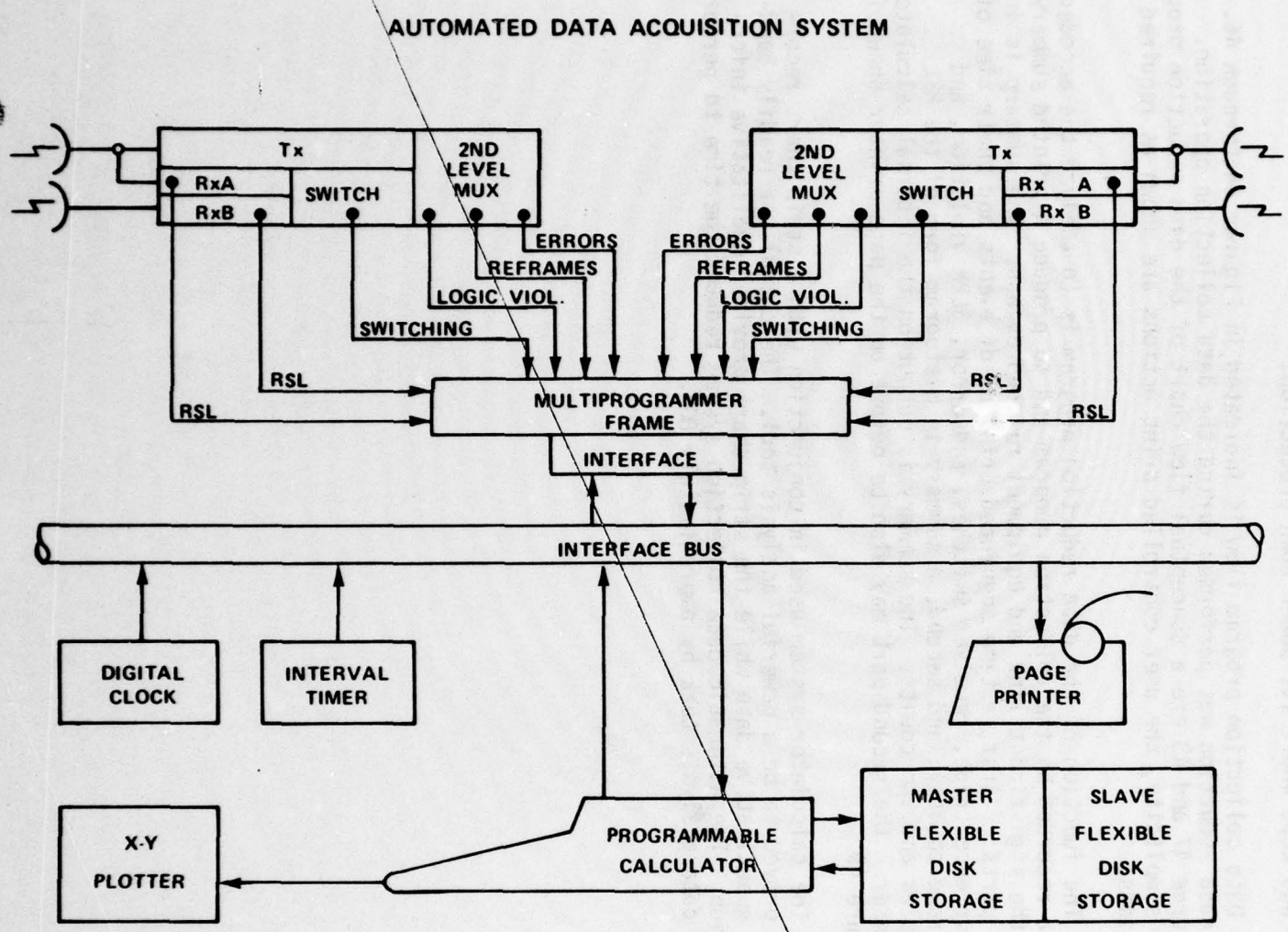

Figure 43. Calculator Interface

the string variable was filled, it was recorded on the mass storage disk system. The string length was chosen as an even number of disk records and was kept short for power down protection.

Data collection program flow is indicated in Figures 44 through 46. No data reduction was performed during the data collection operation. Figures 47 and 48 are a conceptual flow chart of the data reduction program. For simplicity, the user controlled print options are shown as required actions.

The function of the data reduction program is to analyze the encoded data recorded by the collection program and to produce a printed summary of the significant link and equipment related events. The summary is in two parts: first, a time sequenced printout of events and their time of occurrence (fade, receiver switches, and error, 3LPR violation, and reframe counts); and second, a summary in histogram form of the RSL samples and the counts. The summary is output on the internal calculator printer. The second part may also be output on the page printer shown in Figure 49.

The calculator system used in conjunction with a strip chart recorder proved to be a powerful analysis tool. The calculator readily handled quantitative data while the strip chart provided qualitative information. The automatic data collection system reduced the time to perform the data analysis task by approximately 80%.

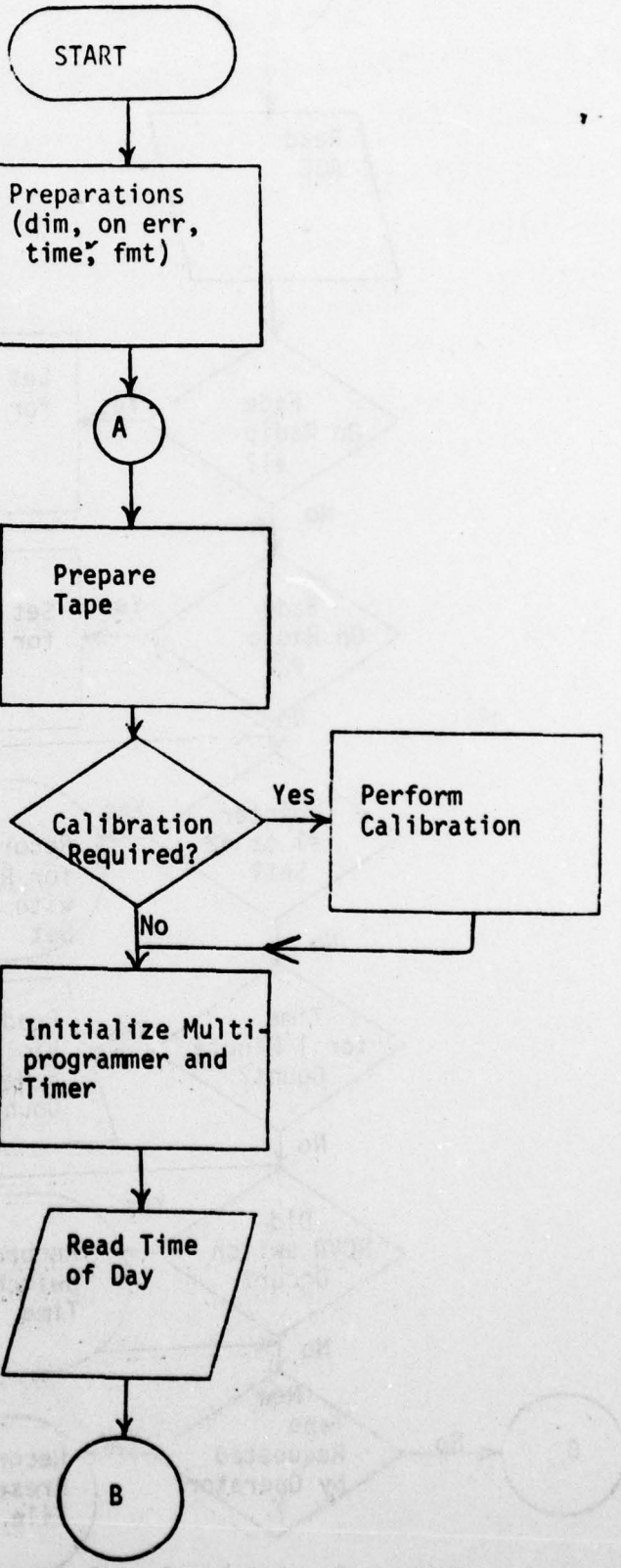

Figure 44. Flow Chart: Data Acquisition Program Part I

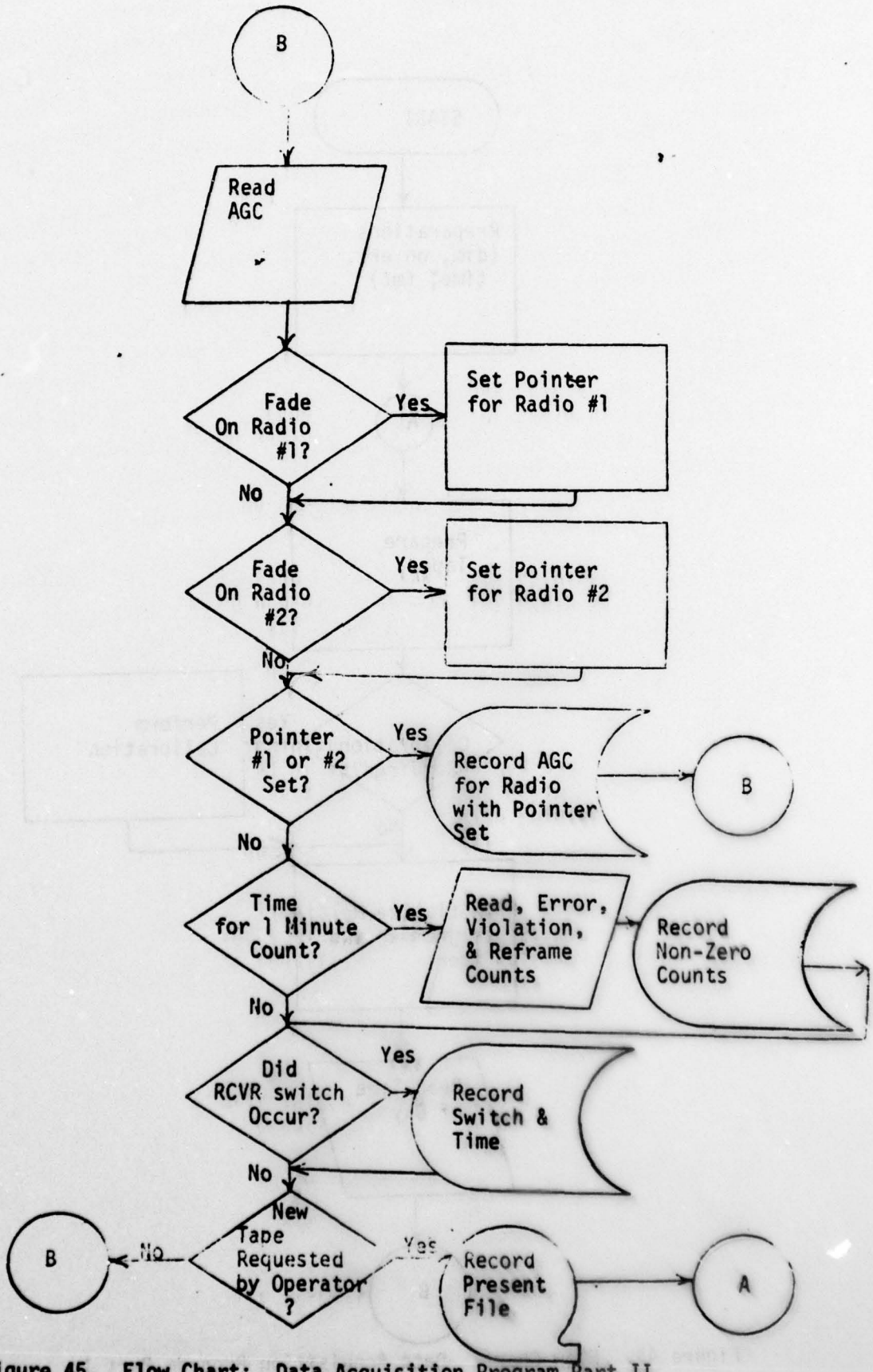

Figure 45. Flow Chart: Data Acquisition Program Part II

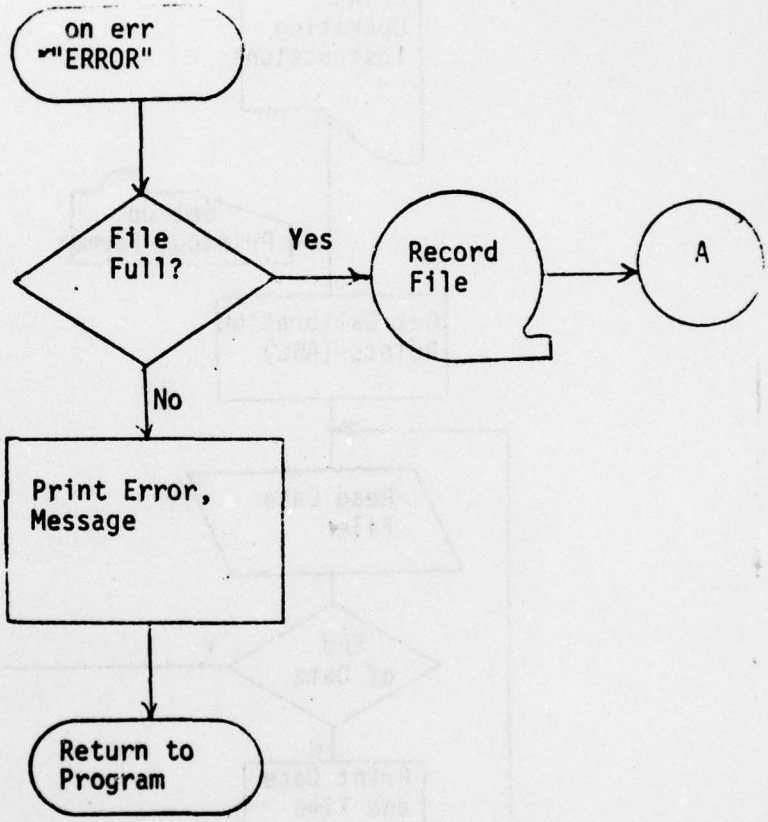

Figure 47. Flow Chart: Data Acquisition Program Part III

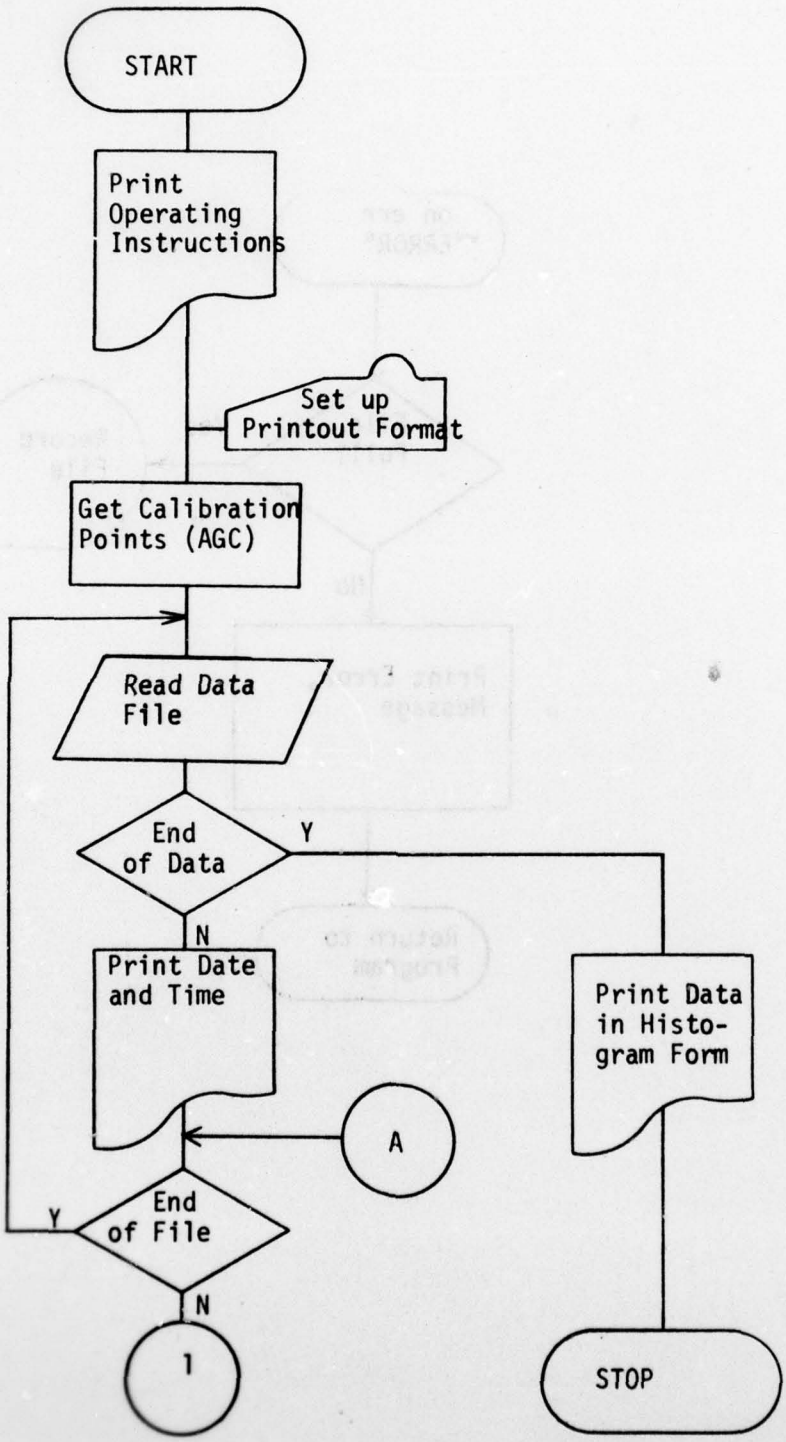

Figure 47. Flow Chart: Data Reduction Program Part I

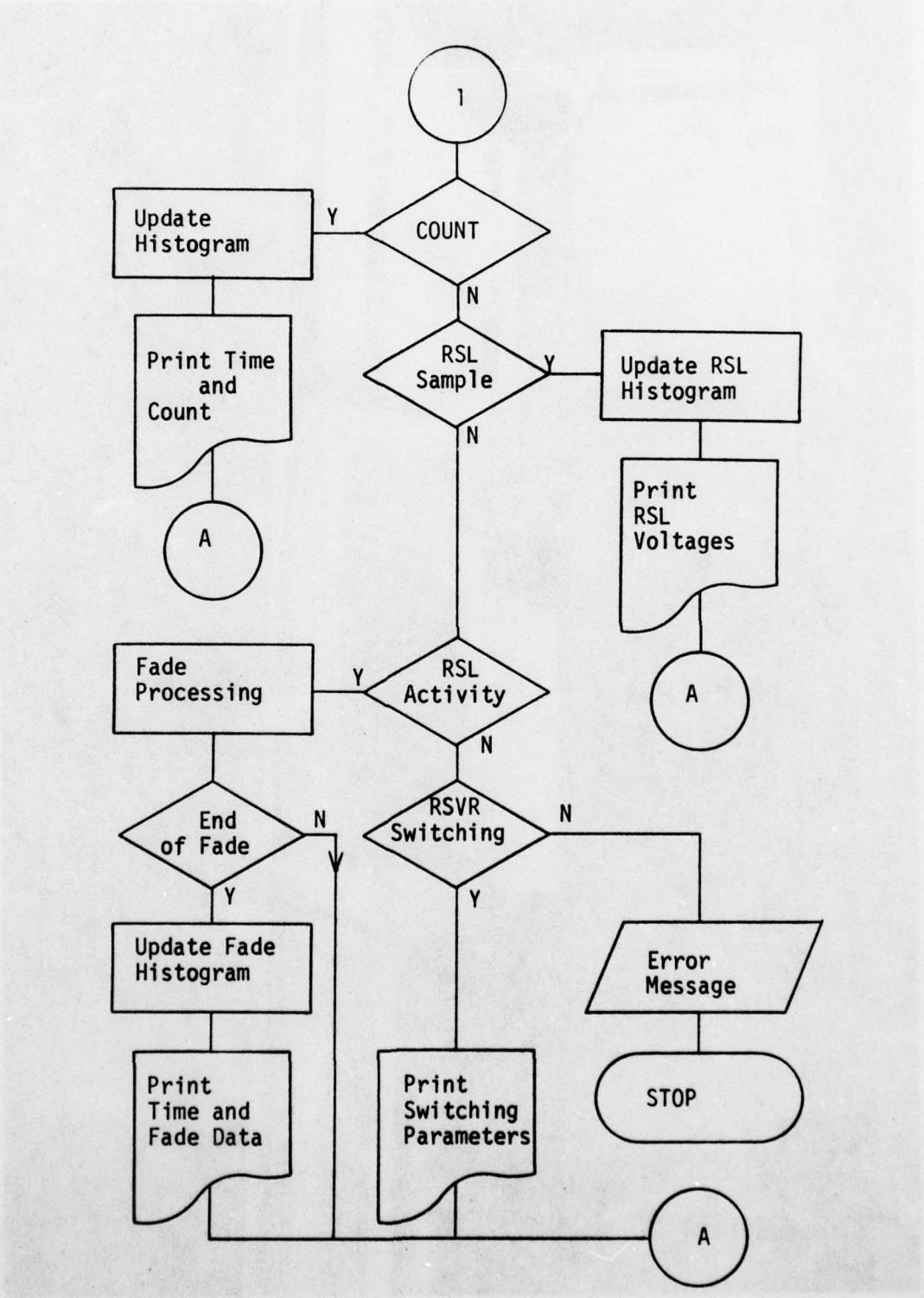

Figure 48. Flow Chart: Data Reduction Program Part II

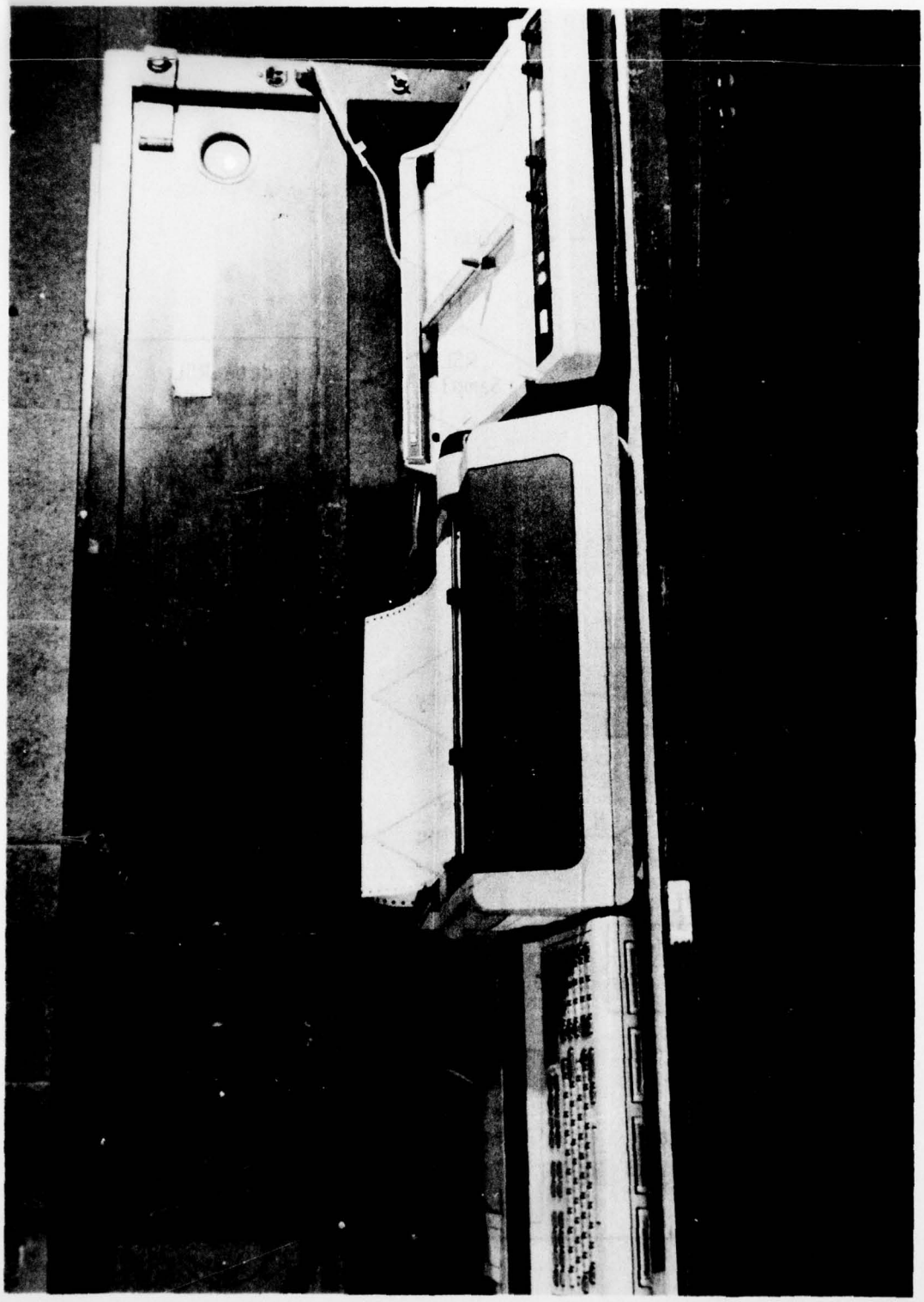

Figure 49. Photograph of Calculator System

DISTRIBUTION	COPIES
AFCS/EPES, Richards Gebaur AFB, MO 64030	2
AFTEC/TEEC, Kirtland AFB, NM 87115	1
CSAF, ATTN: RDPE, Washington, DC 20305	1
ATTN: PRCX, Washington, DC 20305	1
DA/DAMO-TCS-T, Washington, DC 20305	4
DCA, ATTN: NSA Liaison Office, Washington, DC 20305	1
ATTN: 430, Washington, DC 20305	1
ATTN: 470, Washington, DC 20305	1
DCEC, ATTN: R105, 1860 Wiehle Ave, Reston, VA 22070	2
ATTN: R220, 1860 Wiehle Ave, Reston, VA 22070	2
ATTN: R230, 1860 Wiehle Ave, Reston, VA 22070	2
ATTN: R710, 1860 Wiehle Ave, Reston, VA 22070	2
Defense Documentation Center, Alexandria, VA 22314	15
ECAC, ATTN: ACV, Mr. Mager, North Severn, Annapolis, MD 21402	3
Joint Tactical Communications Office,	
ATTN: TT-E-E, 197 Hance Rd, New Shrewsbury, NJ	1
ATTN: TT-E-S, 197 Hance Rd, New Shrewsbury, NJ	1
ATTN: TT-RT-TA, 197 Hance Road, New Shrewsbury, NJ	1
JTO, Tri-Tac, Fort Huachuca, AZ 85613	1
Mitre Corp., P. O. Box 208, ATTN: Mail Stop A160 Bedford, MA 01730	2
National Bureau of Standards, Electromagnetic Division ATTN: W. J. Alspach, Boulder, CO 80302	1
Naval Telecommunications Command,	
ATTN: 3426, Massachusetts Avenue, NW, Wash. DC 20390	1
ATTN: 4401, Massachusetts Avenue, NW, Wash. DC 20390	1
NCA/EPE, Griffis AFB, NY 13440	2
NSA, ATTN: Code R15, Fort Meade, MD 20755	1
ATTN: Code S254, Fort Meade, MD 20755	1
ATTN: Code 4023, Fort Meade, MD 20755	2

RADC, ATTN: DCLD, Griffis AFB, NY 13440	2
ATTN: DCC, Griffis AFB, NY 13440	1
USACC, ATTN: CC-OPS-SM, Fort Huachuca, AZ 85613	4
ATTN: CC-OPS-ST, Fort Huachuca, AZ 85613	2
USACEEIA, ATTN: CCC-CED, Fort Huachuca, AZ 85613	10
ATTN: CCC-TCD, Fort Huachuca, AZ 85613	2
ATTN: CCC-TED, Fort Huachuca, AZ 85613	5
ATTN: CCC-PRSO, Fort Huachuca, AZ 85613	2
USACSA: ATTN: CCM-CCS, Fort Monmouth, NJ 07703	1
ATTN: CCM-SG, Fort Huachuca, AZ 85613	1
ATTN: CCM-RD, Fort Monmouth, NJ 07703	1
US Department of Commerce, Office of Telecommunications, Institute for Telecommunications Sciences, ATTN: Richard Skerjanec, Boulder, CO 80302	2
USAECOM, ATTN: AMSEL-NL-P3, Fort Monmouth NJ 07703	1
ATTN: AMSEL-NL-D, Fort Monmouth, NJ 07703	1
USAEPG/STEEP-MT-GT, Fort Huachuca, AZ 85613	4
ESD, ATTN: DCF Hanscom AFB, Mass 01731	2
Aerospace Corp., P. O. Box 92957, ATTN: J. L. Raymond Bldg A-2, Room 1055 Los Angeles, CA 90009	2